Published for SISSA by Springer

Received: November 17, 2022
Accepted: December 27, 2022
Published: January 26, 2023

Two-loop master integrals for a planar topology contributing to $pp \to t\bar{t}j$

Simon Badger,[a] **Matteo Becchetti,**[a] **Ekta Chaubey**[a,b] **and Robin Marzucca**[c,d]

[a] *Physics Department, Torino University and INFN Torino, Via Pietro Giuria 1, I-10125 Torino, Italy*
[b] *Laboratoire de Physique Théorique et Hautes Energies (LPTHE), UMR 7589, Sorbonne Université et CNRS, 4 place Jussieu, 75252 Paris Cedex 05, France*
[c] *Niels Bohr Institute, Copenhagen University, Blegdamsvej 17, 2100 Copenhagen Ø, Denmark*
[d] *Physik-Institut, Universität Zürich, Winterthurerstrasse 190, 8057 Zürich, Switzerland*

E-mail: simondavid.badger@unito.it, matteo.becchetti@unito.it, ekta@lpthe.jussieu.fr, robin.marzucca@uzh.ch

Abstract: We consider the case of a two-loop five-point pentagon-box integral configuration with one internal massive propagator that contributes to top-quark pair production in association with a jet at hadron colliders. We construct the system of differential equations for all the master integrals in a canonical form where the analytic form is reconstructed from numerical evaluations over finite fields. We find that the system can be represented as a sum of d-logarithmic forms using an alphabet of 71 letters. Using high precision boundary values obtained via the auxiliary mass flow method, a numerical solution to the master integrals is provided using generalised power series expansions.

Keywords: Higher-Order Perturbative Calculations, Top Quark

ArXiv ePrint: 2210.17477

https://doi.org/10.1007/JHEP01(2023)156

JHEP01(2023)156

Contents

JHEP01(2023)156

1 Introduction

As the heaviest particle in the Standard Model (SM) of particle physics, the top quark has many important implications for the nature of the fundamental forces. The stability of the SM vacuum is highly sensitive to the value of the top mass whose precision measurement is a high priority at the Large Hadron Collider (LHC). Top quark pair production at hadron colliders is known extremely precisely both theoretically and experimentally and can be used to constrain SM parameters and parton distribution functions [1, 2]. It has been argued that top-quark pair production in association with a jet is even more sensitive to the value of the top quark mass [3–5], yet the theoretical predictions for this process are not currently at the same level of precision as the experimental measurements. Current theoretical predictions are represented by the next-to-leading order (NLO) QCD corrections [6, 7] with state-of-the-art predictions including complete decay information and interfaces with a parton shower [8–12]. Mixed QCD and EW corrections are now also available [13]. In order to match the experimental precision, see for example [14, 15], next-to-next-to-leading order

(NNLO) corrections are required. Indeed, fully differential cross-section predictions at NNLO in the strong coupling would open up opportunities for the most precise determination of the top-quark mass, yet substantial computational bottlenecks remain.

The two-loop scattering amplitudes that form part of the NNLO correction are currently unknown. In general, amplitudes with massive internal propagators represent a considerable increase in complexity compared to the massless internal propagators that have been considered so far for five particle processes. In addition to the growth in algebraic complexity that comes from the increased number of scales, the analytic complexity contained in the Feynman integrals that appear can lead to difficulties in identifying a numerically well-defined function space. In some cases, of which $pp \to t\bar{t}$ is one, analytic evaluation of the integrals leads to elliptic integrals that still require a better mathematical understanding. While in the case of leading colour $pp \to t\bar{t}j$ elliptic functions should not appear,[1] the evaluation of the master integrals is still a substantial challenge.

A lot of experience in these type of problems has been gained from the study of massless propagator five-point integrals which form a good starting point for the integrals we study in this article. The kinematic case of five massless external particles has now been fully classified into a basis numerically well-defined pentagon functions [16–21]. For the case of one off-shell external leg and four massless legs the situation is also almost complete with the planar [22–24] and the non-planar hexa-box [25] now known. This progress has allowed the calculation of several five-point two-loop scattering amplitudes [16, 19, 26–41] and led to the first NNLO theoretical predictions for $2 \to 3$ processes [42–46].

In this article we make a small step towards the two-loop amplitudes for $pp \to t\bar{t}j$ by considering the computation of the master integrals associated to a five-point pentagon-box configuration with one internal massive propagator (see figure 1). This builds upon previous work considering the one-loop helicity amplitudes expanded up to $\mathcal{O}(\varepsilon^2)$ in the dimensional regulator. Our methodology to determine a set of master integrals follows by the means of the differential equation method [47, 48]. In particular, we write the system of differential equations in a canonical form [49], where the dependence on the dimensional regulator factorises. The canonical form requires the identification of a uniform transcendental weight (UT) basis of master integrals and the solution to a large system of Integration-by-Parts (IBP) relations [50, 51]. For the later we employ the Laporta algorithm [52] which can be implemented within a numerical framework using finite field arithmetic [53–55]. The derivation of the differential equation system can be implemented entirely within the dataflow graphs provided by the FiniteFlow library [55] allowing us to sidestep traditional limitations due to huge intermediate expressions. The determination of a UT basis also presents a significant challenge and has a significant effect on the simplicity of the differential equation system. While considerable effort has been spent to determine automated, or semi-automated techniques for the determination of UT bases yet they are still difficult to apply to situations with a large number of kinematic scales. In this work we will describe

[1] We refrain from making a stronger statement though the pattern established in $pp \to t\bar{t}$ would mean elliptic curves (and more complicated geometries) would only appear in closed heavy fermion loops or sub-leading colour, non-planar topologies.

JHEP01(2023)156

how the UT system can instead be inferred by observing patterns in known examples to provide a suitable ansatz.

Once the differential equation system has been determined we employ the semi-analytic approach to provide the solution of the master integrals. The generalised power series method [56–58] provides a practical way to evaluate the integrals at given numerical values through contour integration from a boundary point. In this work we use the implementation of the method discussed in the ref. [58] into the MATHEMATICA package DIFFEXP [59]. For a successful implementation the boundary value must be given with a sufficiently high numerical precision. The development of the auxiliary mass flow method [60–62] and in particular the MATHEMATICA package AMFLOW [63] offers a simple and practical solution to this task. We are therefore able to offer a solution for the master integrals which has the potential for phenomenological applications, as has been done for other processes [22, 25, 64–70].

Beyond our semi-analytic solution for the master integrals, we also derive the analytic representation for the system of differential equations in terms of logarithmic one-forms. The alphabet for this system is written in a compact form and it shows the same analytic structure as in the five-point massless [16] and in the one-mass [22] cases. As a consequence, this paper lays the groundwork for a fully analytic solution, in terms of an extension of the pentagon functions [18, 21, 24], to the case of top-pair plus jet production.

The paper is structured as follows. In section 2 we define the topology that is under study and we discuss the computational framework. In section 3 we describe our approach to construct the canonical differential equations and the UT basis of master integrals. In section 4 we present the logarithmic one-forms representation of the differential equations and the analytic form of the alphabet, while in section 5 we discuss the numerical evaluation of the master integrals. Finally in 6 we give our conclusions and we analyse future developments.

2 Notation and definitions

We consider the Feynman integral topology in $d = 4 - 2\varepsilon$ dimensions with eight propagators as shown in figure 1. This can be written as,

$$I^{a_9,a_{10},a_{11}}_{a_1,a_2,a_3,a_4,a_5,a_6,a_7,a_8} = \int \mathcal{D}^{4-2\epsilon}k_1 \mathcal{D}^{4-2\epsilon}k_2 \frac{D_9^{a_9} D_{10}^{a_{10}} D_{11}^{a_{11}}}{D_1^{a_1} \cdots D_8^{a_8}} \tag{2.1}$$

where $a_1, \cdots, a_{11} \geq 0$. The propagators, and numerators, are defined as

$$\begin{aligned}
&D_1 = k_1^2, && D_2 = (k_1 - p_1)^2 - m_t^2, && D_3 = (k_1 - p_1 - p_2)^2, \\
&D_4 = (k_1 - p_1 - p_2 - p_3)^2, && D_5 = k_2^2, && D_6 = (k_2 - p_5)^2, \\
&D_7 = (k_2 - p_4 - p_5)^2, && D_8 = (k_1 + k_2)^2, && D_9 = (k_1 + p_5)^2, \\
&D_{10} = (k_2 + p_1)^2 - m_t^2, && D_{11} = (k_2 + p_1 + p_2)^2, &&
\end{aligned} \tag{2.2}$$

and the integration measure is:

$$\mathcal{D}^d k_i = \frac{d^d k_i}{i\pi^{\frac{d}{2}}} e^{\varepsilon \gamma_E} \,. \tag{2.3}$$

JHEP01(2023)156

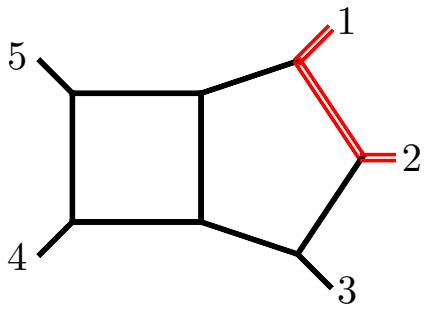

Figure 1. The pentagon-box topology contributing to $pp \to t\bar{t}j$. Black lines denote massless particles and red double-lines denote massive particles.

Momenta are considered outgoing from the graphs and all the particles are on-shell, i.e. $p_1^2 = p_2^2 = m_t^2$ while $p_3^2 = p_4^2 = p_5^2 = 0$. The kinematics of the integrals can be described in terms of six independent invariants. Here we choose the top-quark mass m_t and the five dot products, $\vec{x} = \{d_{12}, d_{23}, d_{34}, d_{45}, d_{15}, m_t^2\}$, where

$$d_{ij} = p_i \cdot p_j. \tag{2.4}$$

The minimal set of master integrals (MIs) is obtained by IBP reduction [51, 71], as implemented in the software LiteRed [72, 73] and FiniteFlow [55]. We found a total number of 88 MIs which are shown in figure 2 and 3.

We wish to find a basis of MIs, $\vec{\mathcal{I}}$, which satisfies a system of differential equations in canonical form [49]:

$$d\vec{\mathcal{I}}(\vec{x}, \varepsilon) = \varepsilon\, dA(\vec{x})\, \vec{\mathcal{I}}(\vec{x}, \varepsilon), \tag{2.5}$$

where d is the total differential with respect to the kinematic invariants, and the matrix $A(\vec{x})$ is a linear combination of logarithms:

$$A(\vec{x}) = \sum c_i \log(w_i(\vec{x})). \tag{2.6}$$

The c_i are matrices of rational numbers, and the *alphabet* $\{w_i(\vec{x})\}$ consists of algebraic functions of the kinematic invariants $\vec{x}$. We discuss the details of the canonical basis of MIs and the alphabet structure in section 3.

The system of differential equations depends on a set of square roots which we define here for later convenience:

$$\begin{aligned}
\beta &= \sqrt{1 - \frac{4m_t^2}{s_{12}}}, \\
\Delta_1 &= \sqrt{\det G(p_{23}, p_1)}, & \Delta_2 &= \sqrt{\det G(p_{15}, p_2)}, \\
\Delta_3 &= \sqrt{1 - \frac{4s_{45}m_t^2}{(s_{12} + s_{23} - m_t^2)^2}}, & \Delta_4 &= \sqrt{1 + \frac{4s_{34}s_{45}m_t^2}{s_{12}(s_{15} - s_{23})^2}}, \\
\Delta_5 &= \sqrt{1 - \frac{s_{45}m_t^2}{4d_{15}d_{23}}}, & \Delta_6 &= \sqrt{1 - \frac{s_{34}s_{45}m_t^2}{4d_{15}d_{23}s_{12}}}, \\
\mathrm{tr}_5 &= 4\sqrt{\det G(p_3, p_4, p_5, p_1)} = \mathrm{tr}(\gamma_5 \not{p}_3 \not{p}_4 \not{p}_5 \not{p}_1),
\end{aligned} \tag{2.7}$$

JHEP01(2023)156

where $G_{ij}(\vec{v}) = v_i \cdot v_j$ is the Gram matrix and $s_{ij} = (p_i + p_j)^2$. The square roots Δ_5 and Δ_6 appear in some intermediate steps of the differential equations reconstruction but they are not related to the normalisation of any master integral. We nevertheless list them here, as some letters of the alphabet can be written in terms of their squared expression and therefore they can be used to match factors appearing in the denominator of the differential equation system.

In order to be able to build a canonical system of differential equations in a rather compact form, our basis of MIs contains integrals with insertions of local numerators [16, 22, 74–76]. We will therefore need to extend the notation introduced in eq. (2.1) to allow for insertions of these local numerators into the integrand. For the scope of this paper it will suffice to extend the notation to the local numerators μ_{ij}, which are defined after splitting the loop momenta into four dimensional and (-2ε) dimensional components,

$$k_i = k_i^{[4]} + k_i^{[-2\varepsilon]}, \qquad \mu_{ij} = -k_i^{[-2\epsilon]} \cdot k_j^{[-2\epsilon]}. \tag{2.8}$$

Hence, we introduce the minimal extensions

$$\begin{aligned} I^{[ij],a_9,a_{10},a_{11}}_{a_1,a_2,a_3,a_4,a_5,a_6,a_7,a_8} &= \int \mathcal{D}^{4-2\epsilon}k_1\, \mathcal{D}^{4-2\epsilon}k_2\, \mu_{ij}\, \frac{D_9^{a_9} D_{10}^{a_{10}} D_{11}^{a_{11}}}{D_1^{a_1} \cdots D_8^{a_8}}\,, \\ I^{[ij,kl],a_9,a_{10},a_{11}}_{a_1,a_2,a_3,a_4,a_5,a_6,a_7,a_8} &= \int \mathcal{D}^{4-2\epsilon}k_1\, \mathcal{D}^{4-2\epsilon}k_2\, \mu_{ij}\, \mu_{kl}\, \frac{D_9^{a_9} D_{10}^{a_{10}} D_{11}^{a_{11}}}{D_1^{a_1} \cdots D_8^{a_8}}\,. \end{aligned} \tag{2.9}$$

3 Canonical form differential equations and a basis of uniform transcendental weight master integrals

In this section we describe the structure of the canonical basis of UT master integrals. The canonical basis approach [49] for systems of differential equations greatly improved the effectiveness of this method for computing Feynman integrals. As a consequence, a great effort has been put into developing techniques aimed at identifying a basis of MIs which satisfy canonical differential equations [49, 77–84]. Given the complexity of the kinematics, automated approaches are difficult to apply in our case yet we find a relatively compact form that demonstrates an emerging pattern in $2 \to 3$ scattering problems [16, 17, 19, 20, 22, 23, 25, 27, 85–87].

Our approach relies on our ability to perform IBP reduction and evaluate the differential equation matrix over finite fields. This means it is relatively easy to extract information about the ε structure of the differential equations from a univariate slice. Combining this with cuts to identify the homogeneous parts of each sector means that it is very quick to check whether particular choices of MIs are suitable. The second important part of our approach is the availability of a sufficiently good set of potential choices. Even though we do not attempt to provide any algorithmic way to generate such a set there is an increasingly large set of known UT bases for $2 \to 3$ scattering problems and many subtopologies that gives us an excellent starting point. In particular the existence of known topologies for massless and one-mass five-point [18, 20, 22, 25] (for e.g. $pp \to W + 2j$ and $pp \to 3j$),

JHEP01(2023)156

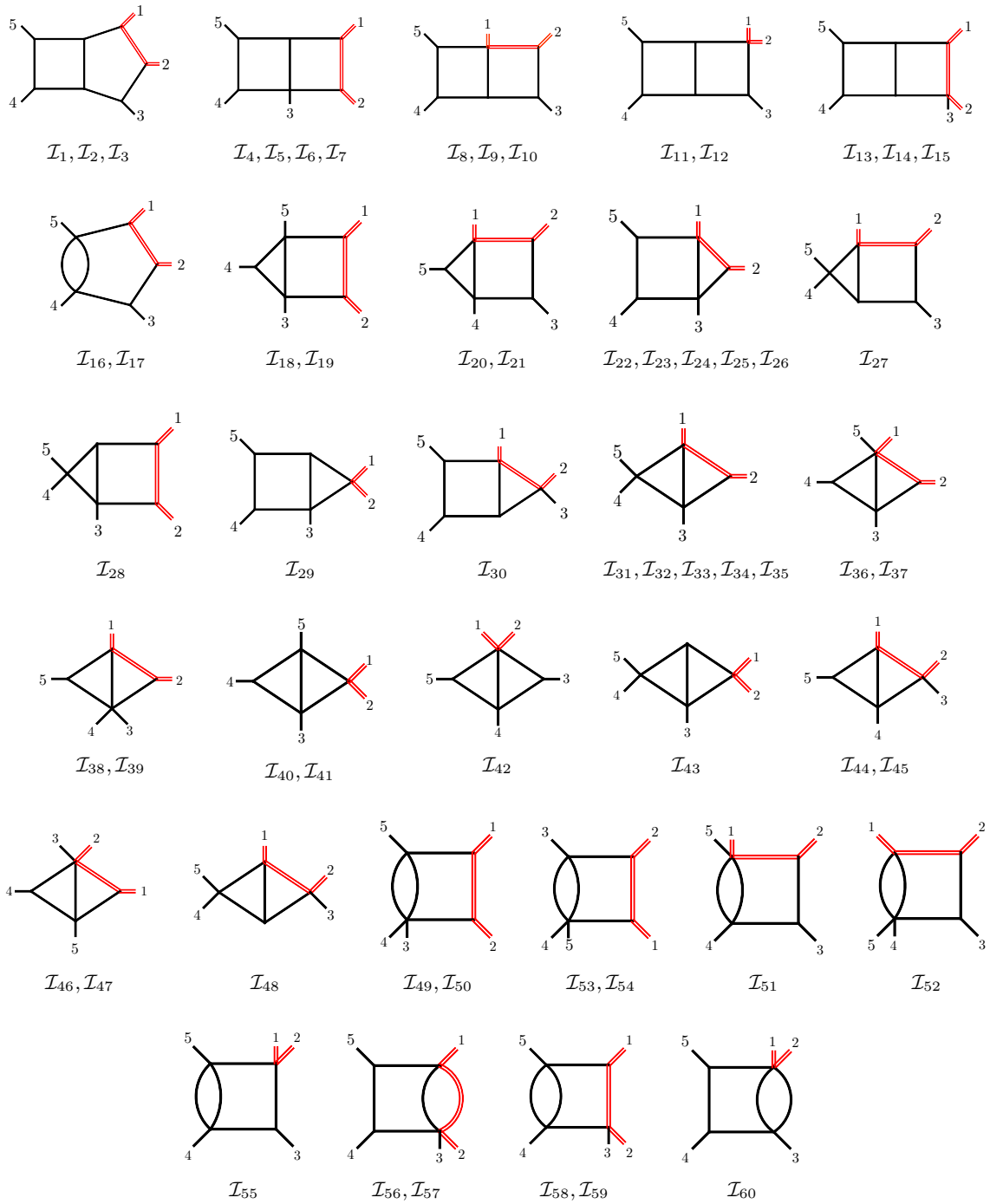

Figure 2. The first 30 diagram topologies describing 60 out of 88 master integrals. The label of the individual sub-figures lists the master integrals belonging to the corresponding topology. Massive propagators and massive external momenta are indicated by red double-lines.

JHEP01(2023)156

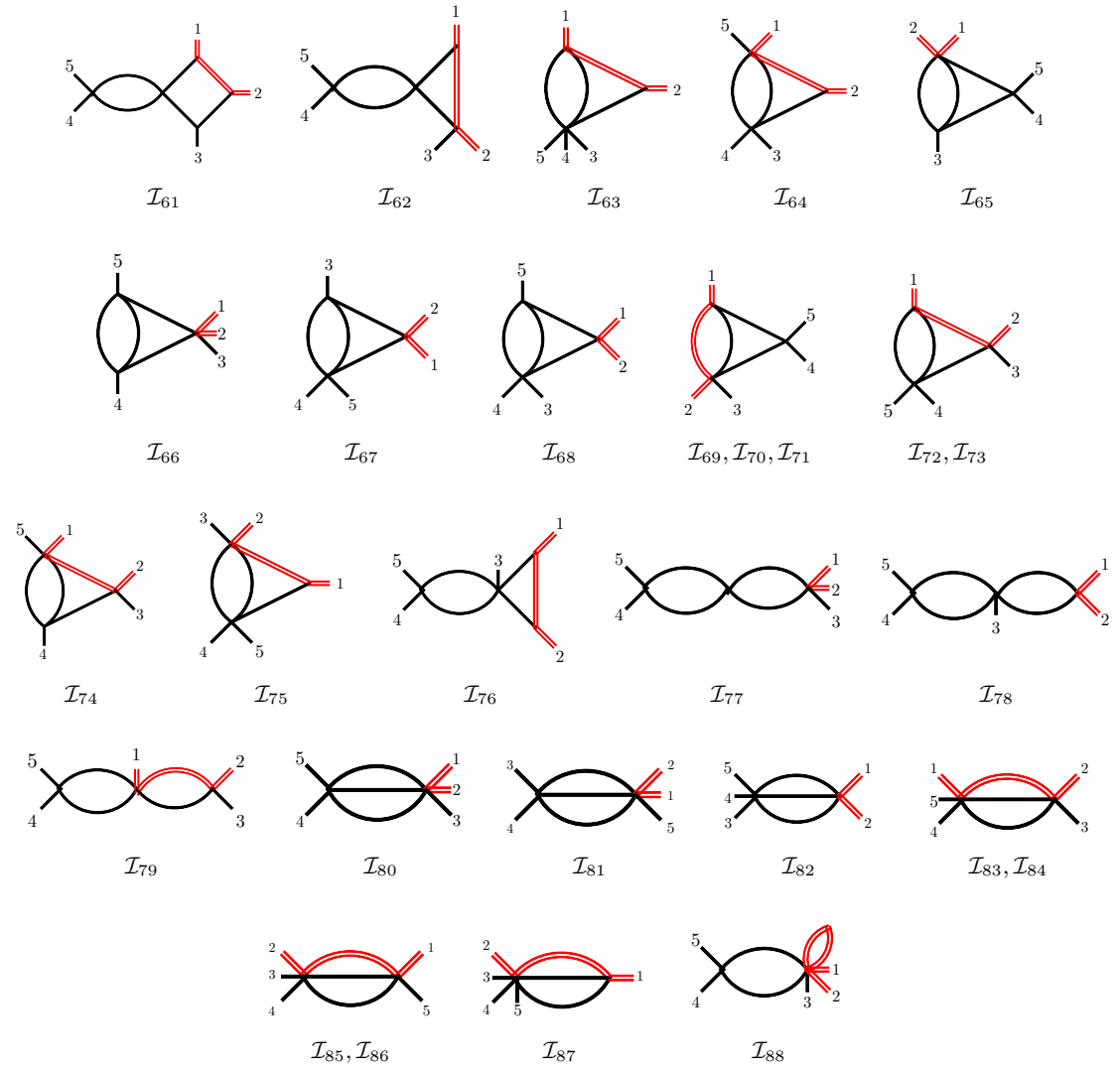

Figure 3. The remaining 23 diagram topologies describing 28 out of 88 master integrals. The label of the individual sub-figures lists the master integrals belonging to the corresponding topology. Massive propagators and massive external momenta are indicated by red double-lines.

two-mass four-point for $pp \to Wt$ scattering [88] provide a lot of information about the subtopologies in our 88 integral system and so only 40 were completely unknown in UT form.

Owing to the large number of square roots appearing in the problem we do not attempt to construct the canonical form of eq. (2.5) directly but instead search for a form linear in ε with purely rational matrices. The square roots appearing in the UT basis can be arranged to be overall normalisations of individual integrals and can thus be removed for the purposes of simple finite field evaluations. This approach is explained in reference [55]. Specifically,

$$d\,\vec{\mathcal{J}}(\vec{x},\varepsilon) = d\,\left(\hat{A}^{(0)}(\vec{x}) + \varepsilon \hat{A}^{(1)}(\vec{x})\right)\,\vec{\mathcal{J}}(\vec{x},\varepsilon), \tag{3.1}$$

where

$$\mathcal{I}_i = N_{ij}(\vec{x})\mathcal{J}_j \tag{3.2}$$

JHEP01(2023)156

and both of the 88×88 matrices $\widehat{A}^{(0)}$ and N are diagonal. The canonical form differential equation is then easy to obtain via,

$$d\,\vec{\mathcal{I}}(\vec{x},\varepsilon) = \varepsilon d\left(N(\vec{x})\widehat{A}^{(1)}(\vec{x})N^{-1}(\vec{x})\right)\,\vec{\mathcal{I}}(\vec{x},\varepsilon) \tag{3.3}$$

after fixing the normalisation through,

$$\widehat{A}^{(0)} - \frac{1}{2}N^2 dN^{(-2)} = 0. \tag{3.4}$$

Since the matrix N is diagonal the inverse and square operations are trivial. We write the latter relations using N^2 to demonstrate it contains only rational functions.

The set of 88 MIs shown in figure 2 and 3 are split into genuine two-loop integrals and one-loop factorisable (one-loop squared) integrals. These integrals are grouped into 52 different sectors of which 6 are of one-loop squared type. We can also subdivide the two-loop topologies by the number of external legs and we will refer to the topologies according to the shape of each loop:

- **Five-point integrals**: this class contains pentagon-box, pentagon-bubble, double-box and box-triangle topologies;
- **Four-point integrals**: this class contains double-box, box-triangle, box-bubble and kite topologies;
- **Three-point integrals**: this class contains kite-like and triangle-bubble topologies;
- **Two-point integrals**: this class contains just the sunrise topology.

The guide for selecting candidate MIs then follows from patterns already observed in previously studied cases and can be justified by considering the leading singularities and local numerator insertions:

- In the two-point and three-point class the canonical MI candidates can involve scalar integrals with dotted denominators;
- In the four-point class the canonical MI candidates can involve scalar integrals with dotted denominators or the numerators D_9, D_{10}, D_{11};
- In the five-point class the canonical MI candidates can involve scalar integrals with the numerators D_9, D_{10}, D_{11} and local integrand insertions μ_{ij}.

Another important feature in the selection of candidates is to ensure that the maximum numerator rank and number of dotted propagators is minimised. Including high rank numerators and large numbers of dotted propagators quickly causes the number of required IBP relations to explode and requires excessive computational resources. We therefore build up from a Laporta style minimisation of numerator rank and dotted denominators and add dots and numerators until each sector has a homogeneous differential equations (i.e. on the maximal cut of each sector) of the form of eq. (3.1). During this process we can also use the univariate slice in ε to determine factorised prefactors that would allow us to rotate

JHEP01(2023)156

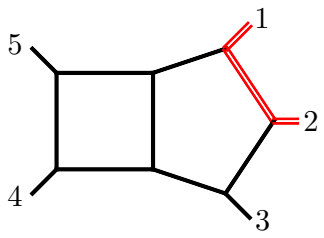

Figure 4. The pentagon-box sector with the master integrals $\mathcal{I}_1$, $\mathcal{I}_2$ and $\mathcal{I}_3$.

the homogeneous differential equation matrix into the desired form. As a result we can use integrals with fewer dots and substitute with prefactors depending only on ε.

After checking each homogeneous system, the remaining ε dependent factors can be determined from a univariate slice of the full system. After this procedure we find that some sectors require additional rotations in sub-sectors. In our case this step was particularly simple and only involved the treatment of 2×2 systems, yet it would be interesting to understand why this is necessary in some cases so a better selection of candidates could be made. Interestingly, such problems did not arise in any of the most complicated five-point topologies where the (extra-dimensional) local numerator insertions worked well.

For the remainder of this section we present explicit forms for all integrals in the five-point sectors. A complete list of the remaining UT integrals is given in appendix A as well as in computer readable form in the supplementary material attached to this paper.

3.1 Pentagon-box sector

The eight propagator pentagon-box sector shown in figure 4 contains three MIs. As the topology with the maximal number of propagators it is particularly important to find a simple basis choice in order to avoid technical complications with the size of the IBP system. In particular we find a convenient choice of UT integrals with a lower tensor rank than in previous five-point bases which simplified the analytic reconstruction.

In these massless and one-mass five-point planar cases [16, 22] a basis of canonical MIs was obtained that involved the following integrals:

$$\left\{ I^{1,0,0}_{1,1,1,1,1,1,1,1,1}, I^{[11,22],0,0,0}_{1,1,1,1,1,1,1,1,1} - I^{[12,12],0,0,0}_{1,1,1,1,1,1,1,1,1}, I^{[12],0,0,0}_{1,1,1,1,1,1,1,1,1} \right\}. \tag{3.5}$$

The local numerator $\mu_{11}\mu_{22} - \mu_{12}^2$, requires the reduction of rank 4 numerators which puts a considerable strain on the system of IBP equations. We find that a different local numerator insertion of rank 2,

$$I^{[11],0,0,0}_{1,1,1,1,1,1,1,1,1}, \tag{3.6}$$

also leads to a UT basis which allows for a simple analytic reconstruction. We note that this choice is also UT for the other five-point configurations mentioned above.

We then find that a canonical basis of MIs for this sector is:

$$\mathcal{I}_1 = \epsilon^4\, 8\, d_{23}\, d_{45} \left(d_{12} + m_t^2\right) I^{1,0,0}_{1,1,1,1,1,1,1,1,1}, \tag{3.7}$$

JHEP01(2023)156

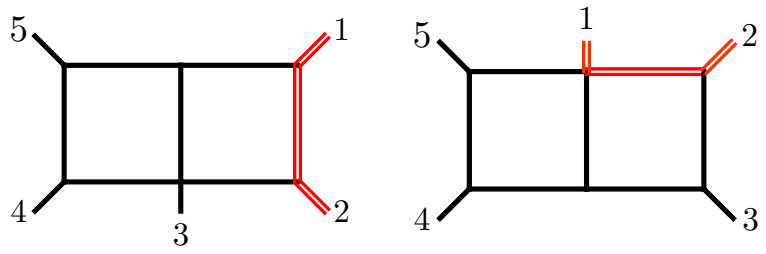

Figure 5. The two five-point double-box topologies, containing the canonical MIs $\mathcal{I}_4$, $\mathcal{I}_5$, $\mathcal{I}_6$, $\mathcal{I}_7$, and $\mathcal{I}_8$, $\mathcal{I}_9$, $\mathcal{I}_{10}$ respectively.

$$\mathcal{I}_2 = \epsilon^4 \frac{d_{45}}{2} \operatorname{tr}_5 I^{[11],0,0,0}_{1,1,1,1,1,1,1,1,1},$$
$$\mathcal{I}_3 = \epsilon^4 \frac{d_{45}}{2} \operatorname{tr}_5 I^{[12],0,0,0}_{1,1,1,1,1,1,1,1,1}\,.$$

One should be aware that this simplification in the rank of the IBP system is only valid for the differential equation system. Rank five numerators cannot, at least with the current technology, be avoided in the reduction of the amplitude. However since the differential equation system requires the reduction of many more dotted propagators than the amplitude, we may still avoid the need for a system requiring simultaneous reduction of high ranks and multiple dots.

3.2 Double-box sectors

There are two sectors with a double-box topology, as shown in figure 5. As for the pentagon-box, a compact form of the canonical basis for these two sectors can be constructed using local numerators. Specifically, we choose as canonical MIs for the first sector in figure 5 the set:

$$\begin{aligned}
\mathcal{I}_4 &= \epsilon^4\, 8\, d_{15}\, d_{45} \left(d_{12} + m_t^2\right) I^{0,0,0}_{1,1,1,0,1,1,1,1,1}, \\
\mathcal{I}_5 &= \epsilon^4\, 4\, \beta\, d_{45} \left(d_{12} + m_t^2\right) I^{1,0,0}_{1,1,1,0,1,1,1,1,1}, \\
\mathcal{I}_6 &= \epsilon^4 \frac{1}{4} \operatorname{tr}_5 I^{[12],0,0,0}_{1,1,1,0,1,1,1,1,1}, \\
\mathcal{I}_7 &= \epsilon^4 \left(d_{12} + m_t^2\right) \left(4\,(d_{15} - d_{23})\, I^{0,0,0}_{1,1,1,0,0,1,1,1} + 4 d_{45} I^{0,1,0}_{1,1,1,0,1,1,1,1}\right).
\end{aligned} \tag{3.8}$$

We note that in the massless limit there are only three master integrals in this sector. The fourth integral in this set was identified by a simple analysis on the maximal cut of the sector, and it required a rotation to remove contribution from a sub-sector. For the second sector in figure 5 we have the following set of canonical MIs:

$$\begin{aligned}
\mathcal{I}_8 &= \epsilon^4\, 4\, d_{23}\, d_{34}\, d_{45}\, I^{0,0,0}_{0,1,1,1,1,1,1,1,1}, \\
\mathcal{I}_9 &= \epsilon^4\, 4\, d_{23}\, d_{45}\, I^{1,0,0}_{0,1,1,1,1,1,1,1,1}, \\
\mathcal{I}_{10} &= \epsilon^4 \frac{1}{4} \operatorname{tr}_5 I^{[12],0,0,0}_{0,1,1,1,1,1,1,1,1}.
\end{aligned} \tag{3.9}$$

These integrals line up precisely with previously considered five-point kinematics.

JHEP01(2023)156

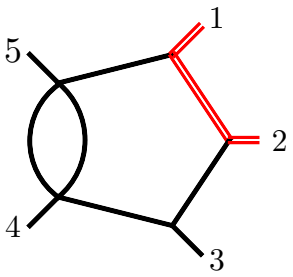

Figure 6. The pentagon with a bubble insertion covers the master integrals $\mathcal{I}_{16}$ and $\mathcal{I}_{17}$.

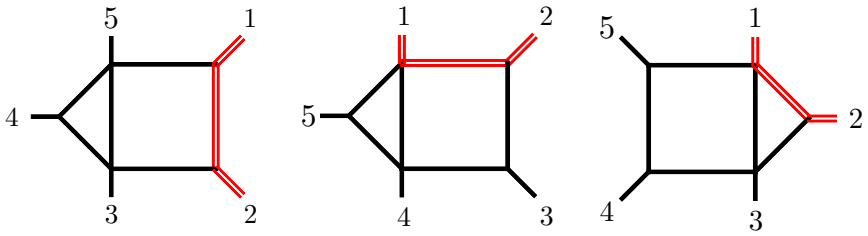

Figure 7. The three genuine five-point box-triangle topologies covering the master integrals $\mathcal{I}_{18}$ and $\mathcal{I}_{19}$ (a), $\mathcal{I}_{20}$ and $\mathcal{I}_{21}$ (b), and $\mathcal{I}_{22}$–$\mathcal{I}_{26}$ (c), respectively.

3.3 Pentagon-bubble sector

For the pentagon-bubble sector, differently from the previous cases, we find a choice of canonical basis which involves also a dotted denominator. The dotted denominator corresponds to one of the one-loop bubble propagators. Hence, we define the canonical basis for this sector as follows:

$$\begin{aligned}\mathcal{I}_{16} &= \epsilon^3(1-2\epsilon)\,4\,d_{23}\left(d_{12}+m_t^2\right) I^{0,0,0}_{1,1,1,1,0,1,0,1},\\ \mathcal{I}_{17} &= \epsilon^3\frac{1}{4}\,\mathrm{tr}_5\, I^{[11],0,0,0}_{1,1,1,1,0,1,0,2}.\end{aligned} \tag{3.10}$$

3.4 Box-triangle sectors

There are three distinct box-triangle sectors with genuine five-point kinematics displayed in figure 7. Four of the nine master integrals require the insertion of local numerators. The explicit form of the canonical MIs in these topologies is given by

$$\begin{aligned}\mathcal{I}_{18} &= \epsilon^4\left(d_{15}-d_{23}\right)\left(d_{12}+m_t^2\right)\Delta_4\, I^{0,0,0}_{1,1,1,0,0,1,1,1},\\ \mathcal{I}_{19} &= \epsilon^3\frac{1}{4}\,\mathrm{tr}_5\, I^{[11],0,0,0}_{1,1,1,0,0,1,1,2},\\ \mathcal{I}_{20} &= \epsilon^4 d_{23}\left(d_{12}-d_{34}+m_t^2\right) I^{0,0,0}_{0,1,1,1,1,1,0,1},\\ \mathcal{I}_{21} &= \epsilon^3\frac{1}{4}\,\mathrm{tr}_5\, I^{[11],0,0,0}_{0,1,1,1,1,1,0,2},\end{aligned} \tag{3.11}$$

JHEP01(2023)156

$$
\begin{aligned}
\mathcal{I}_{22} &= \epsilon^4 d_{45}\, \Delta_2\, I^{0,0,0}_{0,1,1,0,1,1,1,1}, \\
\mathcal{I}_{23} &= \epsilon^3 d_{34}\, d_{45}\, m_t^2\, I^{0,0,0}_{0,2,1,0,1,1,1,1} - \epsilon^4\, (d_{15} - d_{34})\, d_{45}\, I^{0,0,0}_{0,1,1,0,1,1,1,1}, \\
\mathcal{I}_{24} &= \epsilon^3 d_{45}\, m_t^2\, I^{0,0,1}_{0,2,1,0,1,1,1,1} + \epsilon^3 d_{34}\, d_{45}\, m_t^2\, I^{0,0,0}_{0,2,1,0,1,1,1,1} \\
&\quad - 3\,\epsilon^4\, (d_{15} - d_{34})\, d_{45}\, I^{0,0,0}_{0,1,1,0,1,1,1,1}, \\
\mathcal{I}_{25} &= \epsilon^3 \frac{1}{4}\, \mathrm{tr}_5\, I^{[12],0,0,0}_{0,1,1,0,1,1,1,2}, \\
\mathcal{I}_{26} &= \epsilon^3 \frac{1}{4}\, \mathrm{tr}_5\, I^{[22],0,0,0}_{0,1,1,0,1,1,1,2}.
\end{aligned}
$$

3.5 Rational function reconstruction

Having identified an integral basis in the form of eq. (3.1), we find the maximal polynomial degree (numerators/denominators) in the variables ε and d_{ij} drop from 53/57 to 15/15. Since many denominators align with the one-loop case considered recently [70], matching factors on a univariate slice also simplifies the final analytic reconstruction which was eventually achieved in just a couple of hours on a 32 (physical) core workstation.

4 Analytic structure of the differential equations

The reconstructed, ε-factorised form of the DEQ system can be used directly in the generalised series expansion method. However, for a more detailed understanding and the first steps towards constructing a well defined special function basis, we demonstrate that the system can also be written compactly in terms of d-logarithmic forms using an alphabet which is made of 71 letters w_i:

$$
d\vec{\mathcal{I}}(\vec{x},\varepsilon) = \varepsilon\, dA(\vec{x})\, \vec{\mathcal{I}}(\vec{x},\varepsilon), \quad A(\vec{x}) = \sum_{i=1}^{71} c_i \log(w_i(\vec{x})). \tag{4.1}
$$

In situations such as these where there are many square roots it can be difficult to identify the complete alphabet but we find the following a strategy along the lines of those described in refs. [89–91] is sufficient in this case. We proceed in two steps, first we identify a set of rational letters (i.e. without square roots). The remaining algebraic letters containing square roots can then be constructed by examining the denominator structure of a particular element of the total derivative matrix. It is useful to first determine the linear relations in the total derivative matrix to minimise the number of times the strategy must be followed. Given an independent entry of the derivative matrix one looks for all square roots appearing in the denominators. One can then construct an ansatz containing free polynomials in the variables d_{ij} which depends on the number of square roots. If there is one square root we may try a letter of the form,

$$
\Omega(a,b) := \frac{a+\sqrt{b}}{a-\sqrt{b}}, \tag{4.2}
$$

and in the case of two square roots,

$$
\tilde{\Omega}(a,b,c) := \frac{(a+\sqrt{b}+\sqrt{c})(a-\sqrt{b}-\sqrt{c})}{(a+\sqrt{b}-\sqrt{c})(a-\sqrt{b}+\sqrt{c})}. \tag{4.3}
$$

JHEP01(2023)156

Such forms have appeared in numerous of previously studied examples including five-particle kinematics [18, 22, 25, 92]. We note that one can expand the form of eq. (4.3) into one similar to eq. (4.2) where the single square root is the product $\sqrt{bc}$. The structure in eq. (4.3) is preferable as the polynomial degree of the unknown element a is lower as noted in ref. [22]. Using an ansatz for a up to a particular order it is simple to compute the quantity $d(\log(\Omega))$ and check for a solution in the unknown numerical coefficients in a. Taking the polynomial factors inside the square roots and the dimensions into account allows a simple template to be constructed where the polynomial order is kept as low as possible. We note that if the square root appearing in the letter is tr_5 we may find another compact representation of the form,

$$\mathrm{tr}_{\pm}(ij\cdots k) = \frac{1}{2}\,\mathrm{tr}((1\pm\gamma_5)\not{p}_i\not{p}_j\cdots\not{p}_k). \tag{4.4}$$

As before, this follows the structure identified previously in the literature [22, 25, 92].

Following this strategy we identify an alphabet for our case in which the rational and algebraic letters can be divided into subsets which we describe in turn. For the rational letters we define,

$$\mathbf{W}_R := \mathbf{W}_K \cup \mathbf{W}_T \cup \mathbf{W}_S := \{w_1,\cdots,w_{17}\} \cup \{w_{18},\cdots,w_{25}\} \cup \{w_{26},\cdots,w_{33}\}\,, \tag{4.5}$$

and for the algebraic letters

$$\mathbf{W}_A := \mathbf{W}_{SR-1} \cup \mathbf{W}_{TR} \cup \mathbf{W}_{SR-2} := \{w_{34},\cdots,w_{51}\} \cup \{w_{52},\cdots,w_{60}\} \cup \{w_{61},\cdots,w_{71}\}\,. \tag{4.6}$$

The rational set of letters $\mathbf{W}_R$ is made of linear combinations of the kinematic invariants. However, we can identify three different kind of subsets in $\mathbf{W}_R$. The subset $\mathbf{W}_K$ can be written in terms of the Mandelstam variables $s_{ij} = (p_i + p_j)^2$ and it is defined as:

$$\begin{aligned}\mathbf{W}_K := \Big\{&m_t^2,\, s_{12},\, s_{23},\, s_{34},\, s_{45},\, s_{15},\, s_{35},\, s_{23}-m_t^2,\, s_{14}-m_t^2,\, s_{15}-m_t^2,\, s_{24}-m_t^2,\, s_{25}-m_t^2,\\ &s_{12}-s_{34},\, s_{12}-s_{45},\, s_{12}-s_{35},\, s_{23}-s_{15},\, s_{23}-s_{14}\Big\}\,.\end{aligned} \tag{4.7}$$

The subset $\mathbf{W}_T$ consists of letter that can be written as traces over γ-matrices. Defining,

$$\mathrm{tr}(ij\cdots k) = \mathrm{tr}(\not{p}_i\not{p}_j\cdots\not{p}_k), \tag{4.8}$$

we can then write the 8 letters as,

$$\begin{aligned}\mathbf{W}_T := \{&\mathrm{tr}(4151),\, \mathrm{tr}(4232),\, \mathrm{tr}(5242),\, \mathrm{tr}(3252),\, \mathrm{tr}(32[1+2]4[1+2]2),\, \mathrm{tr}(312312)\\ &\mathrm{tr}(412412),\, \mathrm{tr}(512512)\}\,.\end{aligned} \tag{4.9}$$

Finally, the rational letters that belong to the third subset, $\mathbf{W}_S$, can be related to the roots defined in eq. (2.7):

$$\mathbf{W}_S := \Big\{\beta^2,\, (\Delta_1)^2,\, (\Delta_2)^2,\, 4(d_{12}+d_{23}+m_t^2)^2(\Delta_3)^2,\, (\Delta_5)^2,\, (\Delta_4)^2,\, (\Delta_6)^2,\, \mathrm{tr}_5^2\Big\}\,. \tag{4.10}$$

JHEP01(2023)156

We identity three different classes of algebraic letters which involve square roots of the kinematic invariants. The first class, $\mathbf{W}_{SR-1}$, is made by letters in terms of Ω as defined above in eq. (4.2),

$$
\begin{aligned}
&\mathbf{W}_{SR-1} := \\
&\left\{\Omega(1,\beta^2), \Omega\left(1+\frac{m_t^2(d_{12}-d_{34}+m_t^2)}{d_{15}(d_{12}+m_t^2)},\beta^2\right),\right. \\
&\Omega\left(\frac{d_{12}d_{23}+d_{12}m_t^2+d_{23}m_t^2-d_{45}m_t^2+m_t^4}{d_{23}(d_{12}+m_t^2)},\beta^2\right), \\
&\Omega\left(\frac{d_{12}d_{15}-d_{12}d_{23}+d_{12}d_{45}+d_{15}m_t^2-d_{23}m_t^2-d_{34}m_t^2}{(d_{12}+m_t^2)(d_{15}-d_{23}+d_{45})},\beta^2\right), \Omega\left(d_{23}-d_{45},(\Delta_1)^2\right), \\
&\Omega\left(d_{23}-2d_{15}-d_{45},(\Delta_1)^2\right), \Omega\left(\frac{d_{12}(2d_{23}+m_t^2)+(d_{23}+m_t^2)(d_{23}-d_{45}+m_t^2)}{d_{23}},(\Delta_1)^2\right), \\
&\Omega\left(\frac{d_{23}^2-d_{23}d_{45}-d_{45}m_t^2}{d_{23}},(\Delta_1)^2\right), \Omega\left(d_{15}-d_{34},(\Delta_2)^2\right), \Omega\left(d_{15}-2d_{23}-d_{34},(\Delta_2)^2\right), \\
&\Omega\left(\frac{d_{12}(2d_{15}+m_t^2)+(d_{15}+m_t^2)(d_{15}-d_{34}+m_t^2)}{d_{15}},(\Delta_2)^2\right), \\
&\Omega\left(\frac{d_{15}^2-d_{15}d_{34}-d_{34}m_t^2}{d_{15}},(\Delta_2)^2\right), \Omega\left(1,(\Delta_3)^2\right), \Omega\left(1+\frac{2(d_{15}-d_{23}-d_{34})}{d_{12}+d_{23}+m_t^2},(\Delta_3)^2\right), \\
&\Omega\left(\frac{d_{12}d_{23}+d_{12}m_t^2+d_{23}^2+d_{23}m_t^2-d_{45}m_t^2+m_t^4}{d_{23}(d_{12}+d_{23}+m_t^2)},(\Delta_3)^2\right), \Omega\left(1,(\Delta_4)^2\right), \\
&\left.\Omega\left(\frac{d_{15}+d_{23}}{d_{15}-d_{23}},(\Delta_4)^2\right), \Omega\left(\frac{d_{15}d_{34}-d_{15}d_{45}-d_{23}d_{34}+d_{23}d_{45}+2d_{34}d_{45}}{(d_{15}-d_{23})(d_{34}+d_{45})},(\Delta_4)^2\right)\right\}.
\end{aligned}
\tag{4.11}
$$

The letters associated to the class $\mathbf{W}_{TR}$, contain dependence γ_5 and are of the form defined above in eq. (4.4),

$$
\begin{aligned}
\mathbf{W}_{TR} := \Bigg\{&\frac{\mathrm{tr}_+(5241)}{\mathrm{tr}_-(5241)}, \frac{\mathrm{tr}_+(35[1+2]2)}{\mathrm{tr}_-(35[1+2]2)}, \frac{\mathrm{tr}_+(34[1+2]2)}{\mathrm{tr}_-(34[1+2]2)}, \frac{\mathrm{tr}_-(341542)}{\mathrm{tr}_+(341542)}, \\
&\frac{\mathrm{tr}_+(5142[1+2]4)}{\mathrm{tr}_-(5142[1+2]4)}, \frac{\mathrm{tr}_+(3423[1+2]1)}{\mathrm{tr}_-(3423[1+2]1)}, \frac{\mathrm{tr}_+(5232[1+2]4)}{\mathrm{tr}_-(5232[1+2]4)}, \frac{\mathrm{tr}_+(5143[1+2]1)}{\mathrm{tr}_-(5143[1+2]1)}, \\
&\frac{\mathrm{tr}_+(4151[1+2]5)}{\mathrm{tr}_-(4151[1+2]5)}\Bigg\}.
\end{aligned}
\tag{4.12}
$$

The final class, $\mathbf{W}_{SR-2}$, is made by letters in terms of $\tilde{\Omega}$ as defined above in eq. (4.3),

$$
\begin{aligned}
&\mathbf{W}_{SR-2} := \\
&\left\{\tilde{\Omega}\left(d_{12}+d_{23}-d_{45}+m_t^2,(\Delta_1)^2,(d_{12}+m_t^2)^2\beta^2\right),\right. \\
&\tilde{\Omega}\left(d_{12}+d_{15}-d_{34}+m_t^2,(\Delta_2)^2,(d_{12}+m_t^2)^2\beta^2\right), \\
&\tilde{\Omega}\left(d_{23},(\Delta_3)^2(d_{12}+d_{23}+m_t^2)^2,(d_{12}+m_t^2)^2\beta^2\right),
\end{aligned}
$$

JHEP01(2023)156

$$
\begin{aligned}
&\tilde{\Omega}\left(d_{12}-d_{45}+m_t^2,\,(\Delta_3)^2(d_{12}+d_{23}+m_t^2)^2,\,(\Delta_1)^2\right),\\
&\tilde{\Omega}\left(-((d_{12}+m_t^2)(d_{15}-d_{23}+d_{45})),\,(\Delta_4)^2(d_{12}+m_t^2)^2(d_{15}-d_{23})^2,\,\beta^2\,d_{45}^2(d_{12}+m_t^2)^2\right),\\
&\tilde{\Omega}\left(d_{12}d_{15}-d_{12}d_{23}-d_{15}d_{45}+d_{15}m_t^2-d_{23}m_t^2,\,d_{34}^2\,(\Delta_1)^2,\,\frac{\mathrm{tr}_5^2}{16}\right),\\
&\tilde{\Omega}\left(d_{12}d_{15}-d_{12}d_{23}+d_{15}m_t^2+d_{23}d_{34}-d_{23}m_t^2,\,d_{45}^2\,(\Delta_2)^2,\,\frac{\mathrm{tr}_5^2}{16}\right),\\
&\tilde{\Omega}\left(d_{12}^2+d_{12}(d_{15}+d_{23}-d_{34}-d_{45}+2m_t^2)-(d_{45}-m_t^2)(d_{15}-d_{34}+m_t^2)\right.\\
&\left.+d_{23}(m_t^2-d_{34}),\,(d_{12}+m_t^2)^2(d_{12}-d_{34}-d_{45}+m_t^2)^2\beta^2,\,\frac{\mathrm{tr}_5^2}{16}\right),\\
&\tilde{\Omega}\left(d_{12}(d_{15}-d_{23}-d_{34})-(d_{15}-d_{34})(d_{45}-m_t^2)-d_{23}(d_{34}+m_t^2),\,d_{34}^2(d_{12}+m_t^2)^2\beta^2,\,\frac{\mathrm{tr}_5^2}{16}\right),\\
&\tilde{\Omega}\left(d_{12}(d_{15}-d_{23}-d_{34})+d_{15}(m_t^2-d_{45})-m_t^2(d_{23}+d_{34})+d_{34}d_{45},\right.\\
&\left.d_{34}^2(\Delta_3)^2(d_{12}+d_{23}+m_t^2)^2,\,\frac{\mathrm{tr}_5^2}{16}\right),\\
&\tilde{\Omega}\left(d_{15}d_{45}+d_{23}d_{34}-d_{34}d_{45},\,(\Delta_4)^2(d_{12}+m_t^2)^2(d_{15}-d_{23})^2,\,\frac{\mathrm{tr}_5^2}{16}\right)\Bigg\}.
\end{aligned}
\tag{4.13}
$$

We observe encouraging patterns between these letters and those observed in other five-particle kinematic configurations which suggest a general alphabet for all polylogarihmic two-loop integrals with five legs or fewer can be described with similar letters.

4.1 Symbol level structure

While a completely analytic solution for the master integrals is beyond the scope of this article, using the weight zero terms from the boundary values we are able to construct the symbol of the master integrals [93, 94] by iteratively expanding the canonical form differential equation in ε,

$$
\vec{\mathcal{I}}(\vec{x},\epsilon)=\sum_k \epsilon^k\,\vec{\mathcal{I}}^{(k)}(\vec{x}). \tag{4.14}
$$

At each order the result is obtained by integrating over the previous one:

$$
\vec{\mathcal{I}}^{(k)}(\vec{x})=\int\sum_i c_i\,d\log(w_i(\vec{x}))\,\vec{\mathcal{I}}^{(k-1)}(\vec{x}), \tag{4.15}
$$

where at weight 0, $\vec{\mathcal{I}}^{(0)}$ is just the vector of boundary conditions and it is made of rational numbers. For the system of MIs under study $\vec{\mathcal{I}}^{(0)}$ has the following form:

$$
\begin{aligned}
\vec{\mathcal{I}}^{(0)}=\Big\{&\frac{5}{6},0,0,\frac{5}{24},0,0,\frac{1}{6},\frac{19}{24},\frac{5}{6},0,-1,0,\frac{11}{24},0,\frac{5}{12},\frac{1}{2},0,0,0,0,0,0,\frac{1}{6},\frac{5}{12},0,0,0,0,0,0,0,0,\\
&0,0,-\frac{1}{6},-\frac{1}{6},0,\frac{1}{6},0,0,0,-1,0,0,0,0,0,\frac{1}{6},0,0,-\frac{1}{6},\frac{1}{2},\frac{1}{2},0,-\frac{1}{6},0,1,0,0,\frac{1}{6},1,\\
&\frac{1}{2},0,0,0,\frac{1}{2},\frac{1}{2},\frac{1}{2},\frac{1}{2},\frac{1}{2},0,0,\frac{1}{4},0,0,0,0,0,1,1,0,-\frac{1}{2},-\frac{1}{2},-\frac{1}{2},0,-\frac{1}{2},0,-\frac{1}{2},1,1\Big\}.
\end{aligned}
\tag{4.16}
$$

JHEP01(2023)156

By iterating the expression in eq. (4.15) we can write $\vec{\mathcal{I}}^{(k)}(\vec{x})$ as:

$$\vec{\mathcal{I}}^{(k)}(\vec{x}) = \sum_{i_1,\cdots,i_k} e_{i_1,\cdots,i_k} \int d\log(w_{i_1}(\vec{x})) \cdots d\log(w_{i_k}(\vec{x})), \tag{4.17}$$

where $e_{i_1,\cdots,i_k}$ are given by products of the matrices c_i in eq. (2.6). The expression in eq. (4.17) is not enough to obtain an analytic expression for the MIs, however, it contains analytic information at the integrand level which is encoded in the symbol definition [93, 94]:

$$\mathcal{S}\left[\vec{\mathcal{I}}^{(k)}(\vec{x})\right] = \sum_{i_1,\cdots,i_k} e_{i_1,\cdots,i_k} \left[w_{i_1}(\vec{x}), \cdots, w_{i_k}(\vec{x})\right]. \tag{4.18}$$

Using the information provided in the supplementary material attached to this paper together with the descriptions in the literature [93–95] and some help from the PolyLogTools package [96], it is straightforward to construct explicitly the symbol of the master integrals. This symbol level expression can be used to perform a useful consistency check on our results since it carries information about the discontinuities of the Feynman integrals. The so-called *first entry condition* [97] states that $e_{i_1,\cdots,i_k} = 0$ if the first entry, $w_{i_1}(\vec{x})$, in the symbol (4.18) does not correspond to a physical channel of the topology. Checking this condition for our integrals can be simply stated as expanding the symbol level expression to weight one (logarithmic terms only) and checking that the only discontinuities appear in the invariants,

$$\mathcal{T} = \left\{s_{12},\, s_{23} - m_t^2,\, s_{34},\, s_{45},\, s_{15} - m_t^2\right\}, \tag{4.19}$$

which we have confirmed to be true.

5 Numerical solution of the differential equations

As a proof of concept of our work, we discuss in this section a numerical solution for the system of differential equations associated to the master integrals. The system has been integrated semi-analytically exploiting the generalised power series expansion method [58], as implemented in the package DiffExp [59]. Since we are interested in a numerical evaluation of the master integrals, we integrated the system using high-precision numerical boundary conditions. This evaluation has been done exploiting the auxiliary mass flow method [60–62], by means of the package AMFlow [63]. The boundary values are evaluated at the rational point chosen arbitrarily in the Euclidean region:

$$\vec{x}_0 := \left\{-\frac{2}{17}, -\frac{17}{13}, -\frac{19}{7}, -\frac{23}{5}, -\frac{11}{3}, 1\right\}, \tag{5.1}$$

with a precision of $O(100)$ digits. All the relevant material for the numerical evaluation is given in the supplementary material attached to this paper:

- `anc/DiffExp/boundary_value.m`: a set of numerical boundary conditions;
- `anc/DiffExp/DEQs/d_1.m`: the dlog matrix in the DiffExp format;
- `anc/DiffExp/analytic_continuation.m`: the list of polynomials needed for the analytic continuation;

JHEP01(2023)156

- `anc/DiffExp/DIFFEXP_run.wl`: a MATHEMATICA file for the numerical evaluation of the MIs with DIFFEXP;
- `anc/boundary/run.wl`: an AMFLOW script to generate high-precision boundary conditions.

Our numerical tests with DIFFEXP have not been optimised for a realistic phase-space integration required by phenomenological studies. As a result it is not possible to quote any sensible analysis of the evaluation times since in our tests, all benchmark points were transported from the same Euclidean boundary point. While this was useful to establish that the analytic continuation was performed correctly a different strategy would likely be beneficial during the evaluation of multiple points. It has been shown for other processes that iterating in short steps around an initial high precision grid of evaluations can lead to a highly efficient implementation suitable for phase-space integration [22, 25, 67–69, 98]. High precision boundary terms valid in a particular phase-space region can also easily computed using auxiliary mass flow method if required.

5.1 Benchmark points

We now give some benchmark points for the pentagon-box MIs $\mathcal{I}_1$ and $\mathcal{I}_2$. Interestingly, the third master integral in this sector, $\mathcal{I}_3$, is zero up to and including weight 4 for all the points that we studied.

We consider benchmark points for the physical phase-space region in the scattering channel $45 \to 123$:

$$\mathcal{R} := \left\{ p_1^2 > 0,\, p_2^2 > 0,\, d_{12} > 0,\, d_{15} < 0,\, d_{23} > 0,\, d_{34} < 0,\, d_{45} > 0,\, \mathrm{tr}_5^2 < 0 \right\}. \tag{5.2}$$

In particular we consider the following five points:

$$\begin{aligned}
\vec{x}_1 &= \left\{ \frac{13}{80}, \frac{19}{200}, -\frac{11}{80}, \frac{1}{2}, -\frac{81}{400}, \frac{1}{16} \right\}, \\
\vec{x}_2 &= \left\{ \frac{107}{400}, \frac{7}{200}, -\frac{17}{200}, \frac{1}{2}, -\frac{93}{400}, \frac{1}{16} \right\}, \\
\vec{x}_3 &= \left\{ \frac{91}{400}, \frac{23}{200}, -\frac{21}{200}, \frac{1}{2}, -\frac{77}{400}, \frac{1}{16} \right\}, \\
\vec{x}_4 &= \left\{ \frac{271}{400}, \frac{259}{200}, -\frac{222}{25}, \frac{37}{2}, -\frac{3441}{400}, \frac{1}{16} \right\}, \\
\vec{x}_5 &= \left\{ \frac{271}{400}, \frac{1221}{200}, -\frac{222}{25}, \frac{37}{2}, -\frac{2479}{400}, \frac{1}{16} \right\}.
\end{aligned} \tag{5.3}$$

5.2 Numerical checks

We briefly comment on the numerical checks that we performed in order to validate our results. The numerical checks have been done by comparing the numerical results, obtained with DIFFEXP, with respect to a fully numerical evaluations performed with AMFLOW. We made checks for several values of the kinematic invariants and we found full agreement between the two methods.

JHEP01(2023)156

	$\vec{x}_1$	$\vec{x}_2$	$\vec{x}_3$	$\vec{x}_4$	$\vec{x}_5$
$\mathcal{I}_1^{(0)}$	$\frac{5}{6}$	$\frac{5}{6}$	$\frac{5}{6}$	$\frac{5}{6}$	$\frac{5}{6}$
$\mathcal{I}_1^{(1)}$	$2.1892384 + 4.1887902i$	$3.7462547 + 4.1887902i$	$2.0349747 + 4.1887902i$	$-3.8483012 + 4.1887902i$	$-5.9157644 + 4.1887902i$
$\mathcal{I}_1^{(2)}$	$-4.0886316 + 9.4351407i$	$0.601470 + 16.615964i$	$-4.9774769 + 10.3252137i$	$-2.102532 - 29.186022i$	$9.928524 - 35.681149i$
$\mathcal{I}_1^{(3)}$	$-6.9367835 + 6.1424776i$	$-11.982563 + 29.534555i$	$-21.690194 + 10.540708i$	$-89.442855 + 18.056883i$	$58.305031 + 71.732816i$
$\mathcal{I}_1^{(4)}$	$-51.557014 + 40.311095i$	$-50.707105 + 81.832621i$	$-141.376078 + 1.757813i$	$-51.44856 + 237.86399i$	$-277.01306 + 85.51492i$

Table 1. Benchmark points for the pentagon-box master integrals $\mathcal{I}_1$. $\mathcal{I}_1^{(k)}$ indicates the k-th order term in the ϵ-expansion of the integral.

	$\vec{x}_1$	$\vec{x}_2$	$\vec{x}_3$	$\vec{x}_4$	$\vec{x}_5$
$\mathcal{I}_2^{(0)}$	0	0	0	0	0
$\mathcal{I}_2^{(1)}$	0	0	0	0	0
$\mathcal{I}_2^{(2)}$	0	0	0	0	0
$\mathcal{I}_2^{(3)}$	$0.15787753 - 0.49701005i$	$0.09544126 - 0.39795332i$	$0.23166742 - 0.52220052i$	$0.03401419 - 0.28601824i$	$0.16100404 - 0.57235050i$
$\mathcal{I}_2^{(4)}$	$1.1713578 - 2.2750822i$	$0.8565234 - 1.9943250i$	$1.6259689 - 2.5557664i$	$0.00744603 + 1.08835475i$	$-0.2359265 + 1.8438365i$

Table 2. Benchmark points for the pentagon-box master integrals $\mathcal{I}_2$. $\mathcal{I}_2^{(k)}$ indicates the k-th order term in the ϵ-expansion of the integral.

5.3 Remark on square roots numerical evaluation

We finish this section with a comment about the square root implementation within our DiffExp setup. In order to be able to run DiffExp, the differential equations file has to contain only irreducible square roots. As it can be seen from eq. (2.7) the square roots Δ_3 and Δ_4 contain a perfect square at denominator, hence they are not irreducible. Consequently a replacement rule has to be applied within the DiffExp setup. Specifically, we made the following replacement in generating the differential equations file:

$$\begin{aligned}\Delta_3 &\to \text{sign}(d_{12}+d_{23}+m_t^2)\frac{\sqrt{2\left(d_{12}+d_{23}-d_{45}\right)m_t^2+\left(d_{12}+d_{23}\right)^2+m_t^4}}{d_{12}+d_{23}+m_t^2},\\ \Delta_4 &\to \text{sign}(d_{15}-d_{23})\frac{\sqrt{\left(\left(d_{15}-d_{23}\right)^2+2d_{34}d_{45}\right)m_t^2+d_{12}\left(d_{15}-d_{23}\right)^2}}{\sqrt{d_{12}+m_t^2}(d_{15}-d_{23})}.\end{aligned} \tag{5.4}$$

JHEP01(2023)156

The sign in eq. (5.4) depends on the boundary point that is used within DiffExp. As an example, for the setup that is given in the DiffExp files in the supplementary material the sign is negative both for Δ_3 and Δ_4, because we are using the boundary point $\vec{x}_0$ in eq. (5.1). Moreover, the square roots Δ_3 and Δ_4 appear as normalisation factors in the definition of the UT basis for the MIs 18 and 31. Therefore, in order to have a consistent numerical evaluation of these MIs, the sign prefactors in eq. (5.4) have to be kept into account when generating new sets of boundary conditions.

6 Conclusions

In this article we have considered a set of master integrals required to describe $pp \to t\bar{t}j$ at two-loops in QCD in the planar limit. While we have limited ourselves to a semi-analytic evaluation of the integrals using the method of generalised series expansions, the identification of a 'dlog' representation of the differential equation is the first step towards a well defined special function representation as has been achieved in massless propagator cases [18, 21, 24]. We also observe some simple structure in the choices of UT integrals which we hope will be of use when treating the other planar topologies.

An analytic computation of $pp \to t\bar{t}j$ at two-loops in QCD remains a considerable challenge, yet in the planar limit (excluding corrections from closed heavy fermion loops) the prospects look quite reasonable. Of course, as soon as elliptic curves (or more complicated geometries) become relevant, the problem quickly grows in complexity, both for finding a good choice of MIs and reconstructing the differential equation and by the fact that the space of special functions the integrals evaluate to is often unknown. Nevertheless, the successful application of the generalised series expansion together with the high precision boundary values obtained through the auxiliary mass flow method, offers hope that representations suitable for phenomenological applications may be achievable in the near future.

Beyond the phenomenological applications of this work, the analytic results obtained for the differential equations and the alphabet structure could also be of interest in some more theoretical contexts, such as cluster algebras [99, 100] or recent studies concerning the singularities structure of Feynman integrals [101–103].

Acknowledgments

We thank Simone Zoia and Heribertus Bayu Hartanto for many helpful discussions. This project received funding from the European Union's Horizon 2020 research and innovation programmes *High precision multi-jet dynamics at the LHC* (consolidator grant agreement No 772099), *EWMassHiggs* (Marie Skłodowska Curie Grant agreement ID: 101027658), European Research Council starting grant BOSON 101041109 as well as from the Villum Fonden research grant 00025445.

JHEP01(2023)156

A UT integrals for sectors with few than five external legs

In this section we give explicitly the expressions for the UT basis of the non five-point MIs.

Sector: $\mathcal{I}_{11}$, $\mathcal{I}_{12}$

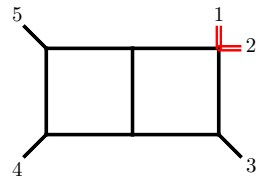

$$\begin{aligned}\mathcal{I}_{11} &= -8d_{34}\,d_{45}^2\,\epsilon^4\,I^{0,0,0}_{1,0,1,1,1,1,1,1}\\ \mathcal{I}_{12} &= -4d_{45}\,(-d_{12}+d_{45}-m_t^2)\,\epsilon^4\,I^{1,0,0}_{1,0,1,1,1,1,1,1}\end{aligned} \tag{A.1}$$

Sector: $\mathcal{I}_{13}$, $\mathcal{I}_{14}$, $\mathcal{I}_{15}$

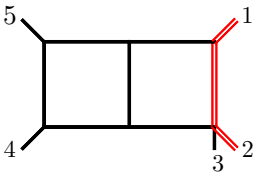

$$\begin{aligned}\mathcal{I}_{13} &= 8d_{15}\,d_{45}^2\,\epsilon^4\,I^{0,0,0}_{1,1,0,1,1,1,1,1}\\ \mathcal{I}_{14} &= 2d_{45}\,\Delta_1\,\epsilon^4\,I^{1,0,0}_{1,1,0,1,1,1,1,1}\\ \mathcal{I}_{15} &= 4d_{45}^2\epsilon^4\,I^{0,1,0}_{1,1,0,1,1,1,1,1}+\frac{3d_{23}\,\epsilon\,(2\epsilon-1)(3\epsilon-2)(3\epsilon-1)}{4d_{15}\,d_{45}}\,I^{0,0,0}_{0,0,0,1,1,0,0,1}\\ &\quad+\frac{4d_{23}\,d_{45}\,m_t^2\,\epsilon^2(2\epsilon-1)}{d_{15}}\,I^{0,0,0}_{1,2,0,1,0,1,0,1}-\frac{4d_{23}\,d_{45}\,m_t^2\,\epsilon^3}{d_{15}}\,I^{0,0,0}_{1,2,0,0,0,1,1,1}\\ &\quad-\frac{\epsilon(2\epsilon-1)(3\epsilon-2)\,(10d_{23}\,\epsilon-2d_{23}+4\epsilon\,m_t^2-m_t^2)}{8d_{15}\,d_{23}}\,I^{0,0,0}_{0,1,0,0,0,0,1,1}\\ &\quad-\frac{3\epsilon^2(2\epsilon-1)(3\epsilon-2)m_t^2}{8d_{15}^2}\,I^{0,0,0}_{0,1,0,0,0,1,0,1}-\frac{3\epsilon^2(2\epsilon-1)(3\epsilon-1)\,(2d_{23}+m_t^2)}{4d_{15}}\,I^{0,0,0}_{0,1,0,1,0,1,0,1}\\ &\quad-\frac{\epsilon(2\epsilon-1)\,(11d_{23}\,\epsilon\,m_t^2-2d_{23}\,m_t^2+4d_{23}^2\,\epsilon+4\epsilon\,m_t^4-m_t^4)}{4d_{15}\,d_{23}}\,I^{0,0,0}_{0,2,0,0,0,0,1,1}\\ &\quad-\frac{3\epsilon^2(2\epsilon-1)m_t^2\,(d_{15}+m_t^2)}{4d_{15}^2}\,I^{0,0,0}_{0,2,0,0,0,1,0,1}+\frac{3d_{23}\,\epsilon^2(2\epsilon-1)(3\epsilon-1)}{2d_{15}}\,I^{0,0,0}_{1,0,0,1,0,1,0,1}\\ &\quad-\frac{6d_{23}\,(d_{15}-d_{23}+d_{45})\,\epsilon^4}{d_{15}}\,I^{0,0,0}_{1,1,0,0,0,1,1,1}-\frac{6d_{23}\,(d_{23}-d_{45})\,\epsilon^3(2\epsilon-1)}{d_{15}}\,I^{0,0,0}_{1,1,0,1,0,1,0,1}\end{aligned} \tag{A.2}$$

Sector: $\mathcal{I}_{27}$

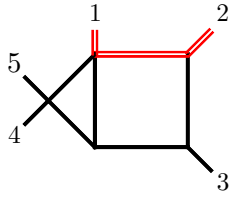

$$\mathcal{I}_{27} = 4d_{23}\,\left(d_{12}-d_{45}+m_t^2\right)\,\epsilon^4\,I^{0,0,0}_{0,1,1,1,1,0,1,1} \tag{A.3}$$

Sector: $\mathcal{I}_{28}$

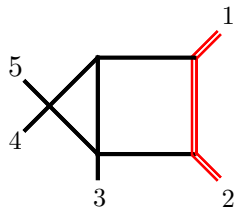

$$\mathcal{I}_{28} = 2\Delta_1 \left(d_{12} + m_t^2\right) \epsilon^4 \, I^{0,0,0}_{1,1,1,0,1,0,1,1} \tag{A.4}$$

Sector: $\mathcal{I}_{29}$

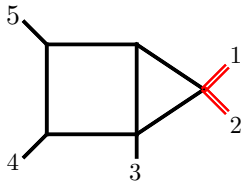

$$\mathcal{I}_{29} = 4d_{45} \left(d_{12} - d_{34} + m_t^2\right) \epsilon^4 \, I^{0,0,0}_{1,0,1,0,1,1,1,1} \tag{A.5}$$

Sector: $\mathcal{I}_{30}$

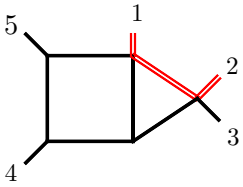

$$\mathcal{I}_{30} = -4\,(d_{15} - d_{23})\; d_{45}\, \epsilon^4 \, I^{0,0,0}_{0,1,0,1,1,1,1,1} \tag{A.6}$$

Sector: $\mathcal{I}_{31}$, $\mathcal{I}_{32}$, $\mathcal{I}_{33}$, $\mathcal{I}_{34}$, $\mathcal{I}_{35}$

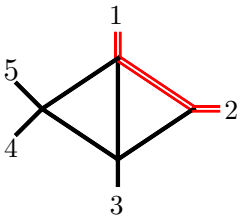

$$\begin{aligned}
\mathcal{I}_{31} &= 2\Delta_3 \left(d_{12} + d_{23} + m_t^2\right) \epsilon^4 \, I^{0,0,0}_{0,1,1,0,1,0,1,1} \\
\mathcal{I}_{32} &= 2m_t^2 \left(d_{12} - d_{45} + m_t^2\right) \epsilon^3 \, I^{0,0,0}_{0,2,1,0,1,0,1,1} \\
\mathcal{I}_{33} &= 4\beta\, d_{45} \left(d_{12} + m_t^2\right) \epsilon^3 \, I^{0,0,0}_{0,1,1,0,2,0,1,1} \\
\mathcal{I}_{34} &= 4d_{23}\, d_{45}\, \epsilon^3 \, I^{0,0,0}_{0,1,1,0,1,0,2,1} \\
\mathcal{I}_{35} &= 4d_{23} \left(d_{12} + m_t^2\right) \epsilon^3 \, I^{0,0,0}_{0,1,1,0,1,0,1,2}
\end{aligned} \tag{A.7}$$

Sectors: $\mathcal{I}_{36}$, $\mathcal{I}_{37}$ **and** $\mathcal{I}_{46}$, $\mathcal{I}_{47}$

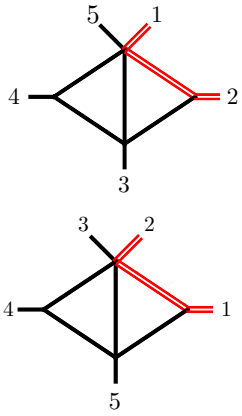

$$\begin{aligned}
\mathcal{I}_{36} &= -2\,(d_{15} - d_{23} - d_{34})\; \epsilon^4 \, I^{0,0,0}_{0,1,1,0,0,1,1,1} \\
\mathcal{I}_{37} &= 2d_{34}\, m_t^2\, \epsilon^3 \, I^{0,0,0}_{0,2,1,0,0,1,1,1} \\
\mathcal{I}_{46} &= 2\,(d_{15} - d_{23} + d_{45})\; \epsilon^4 \, I^{0,0,0}_{1,1,0,0,0,1,1,1} \\
\mathcal{I}_{47} &= 2d_{45}\, m_t^2\, \epsilon^3 \, I^{0,0,0}_{1,2,0,0,0,1,1,1}
\end{aligned} \tag{A.8}$$

JHEP01(2023)156

Sector: $\mathcal{I}_{38}$, $\mathcal{I}_{39}$

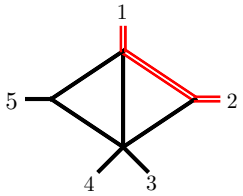

$$\mathcal{I}_{38} = 2\left(d_{12}+d_{15}-d_{34}+m_t^2\right)\,\epsilon^4\,I^{0,0,0}_{0,1,1,0,1,1,0,1}$$
$$\mathcal{I}_{39} = 2m_t^2\,\left(d_{12}-d_{34}+m_t^2\right)\,\epsilon^3\,I^{0,0,0}_{0,2,1,0,1,1,0,1} \tag{A.9}$$

Sector: $\mathcal{I}_{40}$, $\mathcal{I}_{41}$

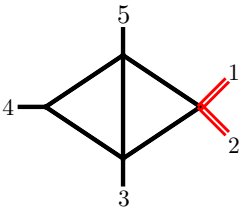

$$\mathcal{I}_{40} = 4\left(d_{34}+d_{45}\right)\,\epsilon^4\,I^{0,0,0}_{1,0,1,0,0,1,1,1}$$
$$\mathcal{I}_{41} = 4d_{34}\,d_{45}\,\epsilon^3\,I^{0,0,0}_{1,0,1,0,0,1,1,2} \tag{A.10}$$

Sector: $\mathcal{I}_{42}$

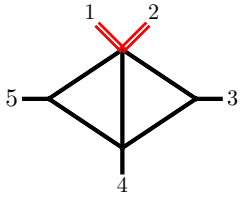

$$\mathcal{I}_{42} = 2\left(d_{12}-d_{34}-d_{45}+m_t^2\right)\,\epsilon^4\,I^{0,0,0}_{0,0,1,1,1,1,0,1} \tag{A.11}$$

Sector: $\mathcal{I}_{43}$

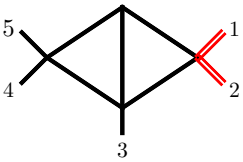

$$\mathcal{I}_{43} = 2\left(d_{12}-d_{45}+m_t^2\right)\,\epsilon^4\,I^{0,0,0}_{1,0,1,0,1,0,1,1} \tag{A.12}$$

Sector: $\mathcal{I}_{44}$, $\mathcal{I}_{45}$

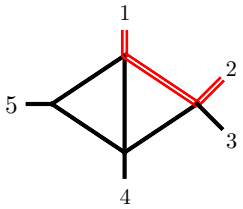

$$\mathcal{I}_{44} = 2\left(d_{15}+d_{45}\right)\,\epsilon^4\,I^{0,0,0}_{0,1,0,1,1,1,0,1}$$
$$\mathcal{I}_{45} = 2\left(2d_{15}d_{23}-d_{45}m_t^2\right)\,\epsilon^3\,I^{0,0,0}_{0,2,0,1,1,1,0,1} \tag{A.13}$$

Sector: $\mathcal{I}_{48}$

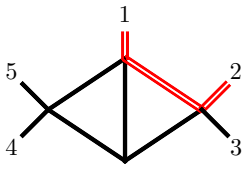

$$\mathcal{I}_{48} = \Delta_1\,\epsilon^4\,I^{0,0,0}_{0,1,0,1,1,0,1,1} \tag{A.14}$$

JHEP01(2023)156

Sectors: $\mathcal{I}_{49}$, $\mathcal{I}_{50}$ **and** $\mathcal{I}_{53}$, $\mathcal{I}_{54}$

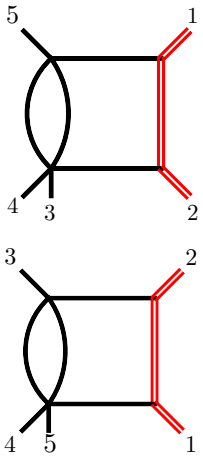

$$\begin{aligned}
\mathcal{I}_{49} &= -2\beta\,(2\epsilon-1)\left(d_{12}+m_t^2\right)\,\epsilon^3\,I^{0,0,0}_{1,1,1,0,0,1,0,1}\\
\mathcal{I}_{50} &= 4d_{15}\,\left(d_{12}+m_t^2\right)\,\epsilon^3\,I^{0,0,0}_{1,1,1,0,0,1,0,2}\\
\mathcal{I}_{53} &= -2\beta\,(2\epsilon-1)\left(d_{12}+m_t^2\right)\,\epsilon^3\,I^{0,0,0}_{1,1,1,0,0,0,1,1}\\
\mathcal{I}_{54} &= 4d_{23}\,\left(d_{12}+m_t^2\right)\,\epsilon^3\,I^{0,0,0}_{1,1,1,0,0,0,1,2}
\end{aligned} \tag{A.15}$$

Sector: $\mathcal{I}_{51}$

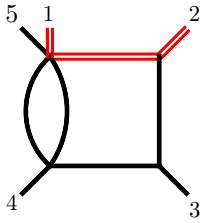

$$\mathcal{I}_{51} = -2d_{23}\,(2\epsilon-1)\,\epsilon^3\,I^{0,0,0}_{0,1,1,1,0,1,0,1} \tag{A.16}$$

Sector: $\mathcal{I}_{52}$

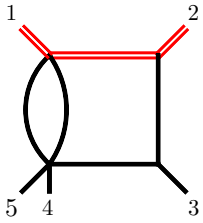

$$\mathcal{I}_{52} = -2d_{23}\,(2\epsilon-1)\,\epsilon^3\,I^{0,0,0}_{0,1,1,1,1,0,0,1} \tag{A.17}$$

Sector: $\mathcal{I}_{55}$

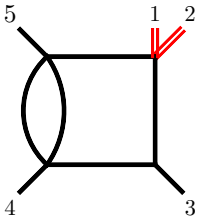

$$\mathcal{I}_{55} = -2(2\epsilon-1)\,\epsilon^3\,\left(d_{12}-d_{45}+m_t^2\right)\,I^{0,0,0}_{1,0,1,1,0,1,0,1} \tag{A.18}$$

JHEP01(2023)156

Sector: $\mathcal{I}_{56}$, $\mathcal{I}_{57}$

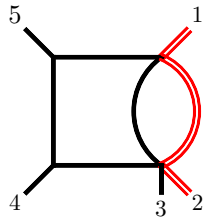

$$\begin{aligned}\mathcal{I}_{56} &= -2d_{45}\,\epsilon^3\,(2\epsilon-1)\,I^{0,0,0}_{0,1,0,0,1,1,1,1}\\ &\quad + 4d_{15}\,d_{45}\,\epsilon^3\,I^{0,0,0}_{0,2,0,0,1,1,1,1}\\ \mathcal{I}_{57} &= 2d_{45}\,\left(2d_{15}+m_t^2\right)\,\epsilon^3\,I^{0,0,0}_{0,2,0,0,1,1,1,1}\end{aligned} \tag{A.19}$$

Sector: $\mathcal{I}_{58}$, $\mathcal{I}_{59}$

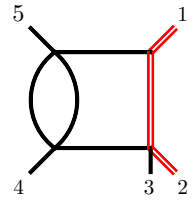

$$\begin{aligned}\mathcal{I}_{58} &= -\Delta_1\,\epsilon^3\,(2\epsilon-1)\,I^{0,0,0}_{1,1,0,1,0,1,0,1}\\ \mathcal{I}_{59} &= \frac{3}{2}\,(d_{23}-d_{45})\,\epsilon^3\,(2\epsilon-1)\,I^{0,0,0}_{1,1,0,1,0,1,0,1}\\ &\quad - d_{45}\,m_t^2\,\epsilon^2\,(2\epsilon-1)\,I^{0,0,0}_{1,2,0,1,0,1,0,1}\end{aligned} \tag{A.20}$$

Sector: $\mathcal{I}_{60}$

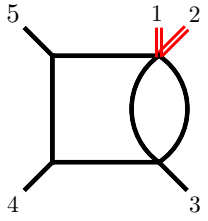

$$\mathcal{I}_{60} = -2d_{45}\,\epsilon^3\,(2\epsilon-1)\,I^{0,0,0}_{0,0,1,0,1,1,1,1} \tag{A.21}$$

Sector: $\mathcal{I}_{61}$

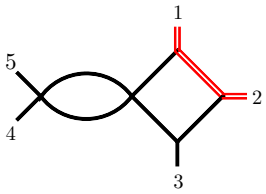

$$\mathcal{I}_{61} = -4d_{23}\,\left(d_{12}+m_t^2\right)\,\epsilon^3\,(2\epsilon-1)\,I^{0,0,0}_{1,1,1,1,1,0,1,0} \tag{A.22}$$

Sector: $\mathcal{I}_{62}$

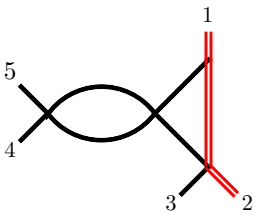

$$\mathcal{I}_{62} = -\Delta_1\,\epsilon^3\,(2\epsilon-1)\,I^{0,0,0}_{1,1,0,1,1,0,1,0} \tag{A.23}$$

JHEP01(2023)156

Sector: $\mathcal{I}_{63}$

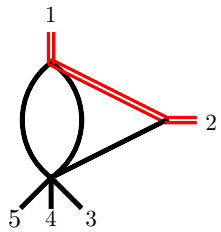

$$\mathcal{I}_{63} = \beta\,\epsilon^2\,(2\epsilon-1)(3\epsilon-1)\,I^{0,0,0}_{0,1,1,0,1,0,0,1} - \frac{\beta\,\epsilon^2\,(2\epsilon-1)(3\epsilon-2)(3\epsilon-1)}{2(4\epsilon-1)\,m_t^2}\,I^{0,0,0}_{0,1,0,0,1,0,0,1} \tag{A.24}$$

Sectors: $\mathcal{I}_{64}$ **and** $\mathcal{I}_{75}$

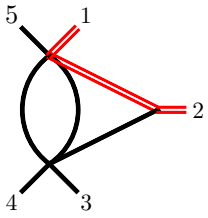

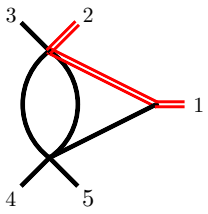

$$\begin{aligned}\mathcal{I}_{64} &= \frac{\Delta_2\,\epsilon^2\,(2\epsilon-1)(3\epsilon-1)}{2d_{34}}\,I^{0,0,0}_{0,1,1,0,0,1,0,1} + \frac{3\Delta_2\,\epsilon^2\,(\epsilon-1)(2\epsilon-1)\,(d_{15}+m_t^2)}{4d_{15}^2\,d_{34}\,m_t^2}\,I^{0,1,0}_{0,1,0,0,0,1,0,1} \\ &\quad - \frac{\Delta_2\,\epsilon^2\,(2\epsilon-1)\,(-5d_{15}\epsilon\,m_t^2+3d_{15}\,m_t^2+2d_{15}^2\,\epsilon-2d_{15}^2-4\epsilon\,m_t^4+3m_t^4)}{4d_{15}^2\,d_{34}\,m_t^2}\,I^{0,0,0}_{0,1,0,0,0,1,0,1} \\ \mathcal{I}_{75} &= \frac{\Delta_1\,\epsilon^2\,(2\epsilon-1)(3\epsilon-1)}{2d_{45}}\,I^{0,0,0}_{1,1,0,0,0,0,1,1} + \frac{\Delta_1\,\epsilon^2\,(2\epsilon-1)(3\epsilon-2)}{4d_{23}\,d_{45}}\,I^{0,0,0}_{0,1,0,0,0,0,1,1} \\ &\quad + \frac{\Delta_1\,\epsilon^2\,(2\epsilon-1)\,(d_{23}+m_t^2)}{2d_{23}\,d_{45}}\,I^{0,0,0}_{0,2,0,0,0,0,1,1}\end{aligned} \tag{A.25}$$

Sector: $\mathcal{I}_{65}$

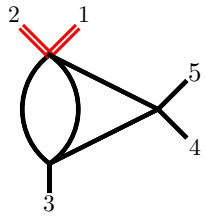

$$\mathcal{I}_{65} = \epsilon^2\,(2\epsilon-1)(3\epsilon-1)\,I^{0,0,0}_{0,0,1,0,1,0,1,1} \tag{A.26}$$

Sector: $\mathcal{I}_{66}$

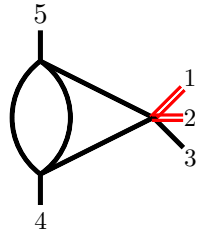

$$\mathcal{I}_{66} = \epsilon^2\,(2\epsilon-1)(3\epsilon-1)\,I^{0,0,0}_{1,0,0,1,0,1,0,1} \tag{A.27}$$

JHEP01(2023)156

Sectors: $\mathcal{I}_{67}$ **and** $\mathcal{I}_{68}$

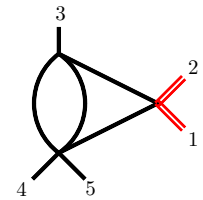

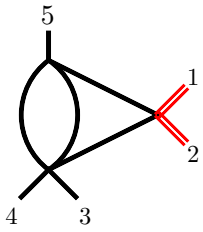

$$\begin{aligned}\mathcal{I}_{67} &= \epsilon^2\,(2\epsilon-1)(3\epsilon-1)\,I^{0,0,0}_{1,0,1,0,0,0,1,1}\\ \mathcal{I}_{68} &= \epsilon^2\,(2\epsilon-1)(3\epsilon-1)\,I^{0,0,0}_{1,0,1,0,0,1,0,1}\end{aligned} \tag{A.28}$$

Sector: $\mathcal{I}_{69}$, $\mathcal{I}_{70}$, $\mathcal{I}_{71}$

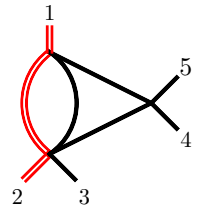

$$\begin{aligned}\mathcal{I}_{69} &= \epsilon^2\,(2\epsilon-1)(3\epsilon-1)\,I^{0,0,0}_{0,1,0,0,1,0,1,1}\\ &\quad -\epsilon^3\,\left(d_{23}-d_{45}\right)\,I^{0,0,0}_{0,1,0,0,1,0,1,2}\\ &\quad +\epsilon^2(4\epsilon-1)\,m_t^2\,I^{0,0,0}_{0,2,0,0,1,0,1,1}\\ \mathcal{I}_{70} &= \Delta_1\,\epsilon^3\,I^{0,0,0}_{0,2,0,0,1,0,1,1}\\ \mathcal{I}_{71} &= \Delta_1\,\epsilon^3\,I^{0,0,0}_{0,1,0,0,1,0,1,2}\end{aligned} \tag{A.29}$$

Sector: $\mathcal{I}_{72}$, $\mathcal{I}_{73}$

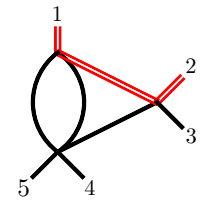

$$\begin{aligned}\mathcal{I}_{72} &= \frac{\epsilon^2\,(2\epsilon-1)(3\epsilon-1)\,(2d_{23}+m_t^2)}{2d_{23}}\,I^{0,0,0}_{0,1,0,1,1,0,0,1}\\ &\quad +\frac{\epsilon^3\,\left(-d_{45}m_t^2+d_{23}^2-d_{45}d_{23}\right)}{d_{23}}\,I^{0,0,0}_{0,1,0,1,1,0,0,2}\\ &\quad -\frac{\epsilon^2\,(2\epsilon-1)(3\epsilon-2)(3\epsilon-1)\,(d_{23}+m_t^2)}{4d_{23}\,m_t^2\,(4\epsilon-1)}\,I^{0,0,0}_{0,1,0,0,1,0,0,1}\\ \mathcal{I}_{73} &= \Delta_1\,\epsilon^3\,I^{0,0,0}_{0,1,0,1,1,0,0,2}\end{aligned} \tag{A.30}$$

Sector: $\mathcal{I}_{74}$

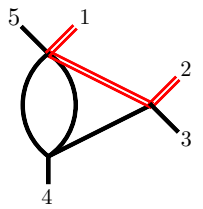

$$\begin{aligned}\mathcal{I}_{74} &= \frac{\epsilon^2\,(2\epsilon-1)(3\epsilon-1)\,(2d_{23}+m_t^2)}{2d_{23}}\,I^{0,0,0}_{0,1,0,1,0,1,0,1}\\ &\quad +\frac{\epsilon^2\,(2\epsilon-1)\,(d_{15}+m_t^2)\,(2d_{23}+m_t^2)}{2d_{15}\,d_{23}}\,I^{0,0,0}_{0,2,0,0,0,1,0,1}\\ &\quad +\frac{\epsilon^2\,(2\epsilon-1)(3\epsilon-2)\,(2d_{23}+m_t^2)}{4d_{15}\,d_{23}}\,I^{0,0,0}_{0,1,0,0,0,1,0,1}\end{aligned} \tag{A.31}$$

JHEP01(2023)156

Sector: $\mathcal{I}_{76}$

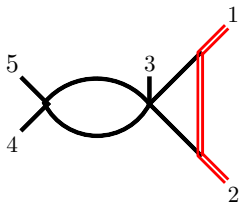

$$\mathcal{I}_{76} = -2\beta\,\epsilon^3\,(2\epsilon-1)\left(d_{12}+m_t^2\right)\,I^{0,0,0}_{1,1,1,0,1,0,1,0} \tag{A.32}$$

Sector: $\mathcal{I}_{77}$

$$\mathcal{I}_{77} = \epsilon^2\,(2\epsilon-1)^2\,I^{0,0,0}_{1,0,0,1,1,0,1,0} \tag{A.33}$$

Sector: $\mathcal{I}_{78}$

$$\mathcal{I}_{78} = \epsilon^2\,(2\epsilon-1)^2\,I^{0,0,0}_{1,0,1,0,1,0,1,0} \tag{A.34}$$

Sector: $\mathcal{I}_{79}$

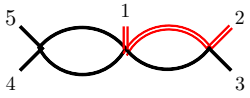

$$\begin{aligned}\mathcal{I}_{79} = &\frac{\epsilon^2\,(2\epsilon-1)^2\,(2d_{23}+m_t^2)}{2d_{23}}\,I^{0,0,0}_{0,1,0,1,1,0,1,0}\\ &-\frac{\epsilon^2\,(\epsilon-1)(2\epsilon-1)\,(2d_{23}+m_t^2)}{2d_{23}\,m_t^2}\,I^{0,0,0}_{0,1,0,0,1,0,1,0}\end{aligned} \tag{A.35}$$

Sectors: $\mathcal{I}_{80}$ **and** $\mathcal{I}_{81}$

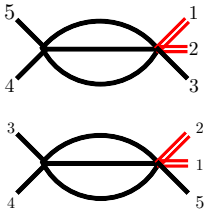

$$\begin{aligned}\mathcal{I}_{80} &= -\frac{\epsilon\,(2\epsilon-1)(3\epsilon-2)(3\epsilon-1)}{2d_{45}}\,I^{0,0,0}_{0,0,0,1,1,0,0,1}\\ \mathcal{I}_{81} &= -\frac{\epsilon\,(2\epsilon-1)(3\epsilon-2)(3\epsilon-1)}{2d_{34}}\,I^{0,0,0}_{0,0,1,0,0,1,0,1}\end{aligned} \tag{A.36}$$

Sector: $\mathcal{I}_{82}$

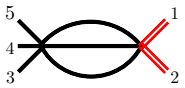

$$\mathcal{I}_{82} = -\frac{\epsilon\,(2\epsilon-1)(3\epsilon-2)(3\epsilon-1)}{2\,(d_{12}+m_t^2)}\,I^{0,0,0}_{0,0,1,0,1,0,0,1} \tag{A.37}$$

JHEP01(2023)156

Sectors: $\mathcal{I}_{83}$, $\mathcal{I}_{84}$ **and** $\mathcal{I}_{85}$, $\mathcal{I}_{86}$

$$\begin{aligned}
\mathcal{I}_{83} &= -\frac{\epsilon\,(2\epsilon-1)(3\epsilon-2)(4\epsilon-1)\,(2d_{23}+m_t^2)}{4d_{23}^2}\,I^{0,0,0}_{0,1,0,0,0,0,1,1} \\
&\quad -\frac{\epsilon\,(2\epsilon-1)\,(2d_{23}+m_t^2)\,(\epsilon\,d_{23}+4\epsilon\,m_t^2-m_t^2)}{2d_{23}^2}\,I^{0,0,0}_{0,2,0,0,0,0,1,1} \\
\mathcal{I}_{84} &= \frac{\epsilon^2\,(2\epsilon-1)(3\epsilon-2)}{2d_{23}}\,I^{0,0,0}_{0,1,0,0,0,0,1,1}+\frac{\epsilon^2\,(2\epsilon-1)\,(d_{23}+m_t^2)}{d_{23}}\,I^{0,0,0}_{0,2,0,0,0,0,1,1} \\
\mathcal{I}_{85} &= -\frac{\epsilon\,(2\epsilon-1)(3\epsilon-2)(4\epsilon-1)\,(2d_{15}+m_t^2)}{4d_{15}^2}\,I^{0,0,0}_{0,1,0,0,0,1,0,1} \\
&\quad -\frac{\epsilon\,(2\epsilon-1)\,(2d_{15}+m_t^2)\,(\epsilon\,d_{15}+4\epsilon\,m_t^2-m_t^2)}{2d_{15}^2}\,I^{0,0,0}_{0,2,0,0,0,1,0,1} \\
\mathcal{I}_{86} &= \frac{\epsilon^2\,(2\epsilon-1)(3\epsilon-2)}{2d_{15}}\,I^{0,0,0}_{0,1,0,0,0,1,0,1}+\frac{\epsilon^2\,(2\epsilon-1)\,(d_{15}+m_t^2)}{d_{15}}\,I^{0,0,0}_{0,2,0,0,0,1,0,1}
\end{aligned} \tag{A.38}$$

Sector: $\mathcal{I}_{87}$

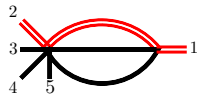

$$\mathcal{I}_{87} = \frac{\epsilon^2\,(2\epsilon-1)(3\epsilon-2)(3\epsilon-1)}{(4\epsilon-1)m_t^2}\,I^{0,0,0}_{0,1,0,0,1,0,0,1} \tag{A.39}$$

Sector: $\mathcal{I}_{88}$

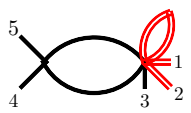

$$\mathcal{I}_{88} = \frac{\epsilon^2\,(\epsilon-1)(2\epsilon-1)}{m_t^2}\,I^{0,0,0}_{0,1,0,0,1,0,1,0} \tag{A.40}$$

References

[1] M. Czakon, S. Dulat, T.-J. Hou, J. Huston, A. Mitov, A.S. Papanastasiou et al., *An exploratory study of the impact of CMS double-differential top distributions on the gluon parton distribution function*, *J. Phys. G* **48** (2020) 015003 [arXiv:1912.08801] [INSPIRE].

[2] A.M. Cooper-Sarkar, M. Czakon, M.A. Lim, A. Mitov and A.S. Papanastasiou, *Simultaneous extraction of α_s and m_t from LHC $t\bar{t}$ differential distributions*, CAVENDISH-HEP-20/12 [arXiv:2010.04171] [INSPIRE].

[3] S. Alioli, P. Fernandez, J. Fuster, A. Irles, S.-O. Moch, P. Uwer et al., *A new observable to measure the top-quark mass at hadron colliders*, *Eur. Phys. J. C* **73** (2013) 2438 [arXiv:1303.6415] [INSPIRE].

JHEP01(2023)156

[4] G. Bevilacqua, H.B. Hartanto, M. Kraus, M. Schulze and M. Worek, *Top quark mass studies with $t\bar{t}j$ at the LHC*, *JHEP* **03** (2018) 169 [arXiv:1710.07515] [INSPIRE].

[5] S. Alioli, J. Fuster, M.V. Garzelli, A. Gavardi, A. Irles, D. Melini et al., *Phenomenology of $t\bar{t}j$ + X production at the LHC*, *JHEP* **05** (2022) 146 [arXiv:2202.07975] [INSPIRE].

[6] S. Dittmaier, P. Uwer and S. Weinzierl, *NLO QCD corrections to $t\bar{t}$ + jet production at hadron colliders*, *Phys. Rev. Lett.* **98** (2007) 262002 [hep-ph/0703120] [INSPIRE].

[7] S. Dittmaier, P. Uwer and S. Weinzierl, *Hadronic top-quark pair production in association with a hard jet at next-to-leading order QCD: Phenomenological studies for the Tevatron and the LHC*, *Eur. Phys. J. C* **59** (2009) 625 [arXiv:0810.0452] [INSPIRE].

[8] K. Melnikov and M. Schulze, *NLO QCD corrections to top quark pair production in association with one hard jet at hadron colliders*, *Nucl. Phys. B* **840** (2010) 129 [arXiv:1004.3284] [INSPIRE].

[9] S. Alioli, S.-O. Moch and P. Uwer, *Hadronic top-quark pair-production with one jet and parton showering*, *JHEP* **01** (2012) 137 [arXiv:1110.5251] [INSPIRE].

[10] M. Czakon, H.B. Hartanto, M. Kraus and M. Worek, *Matching the Nagy-Soper parton shower at next-to-leading order*, *JHEP* **06** (2015) 033 [arXiv:1502.00925] [INSPIRE].

[11] G. Bevilacqua, H.B. Hartanto, M. Kraus and M. Worek, *Top Quark Pair Production in Association with a Jet with Next-to-Leading-Order QCD Off-Shell Effects at the Large Hadron Collider*, *Phys. Rev. Lett.* **116** (2016) 052003 [arXiv:1509.09242] [INSPIRE].

[12] G. Bevilacqua, H.B. Hartanto, M. Kraus and M. Worek, *Off-shell Top Quarks with One Jet at the LHC: A comprehensive analysis at NLO QCD*, *JHEP* **11** (2016) 098 [arXiv:1609.01659] [INSPIRE].

[13] C. Gütschow, J.M. Lindert and M. Schönherr, *Multi-jet merged top-pair production including electroweak corrections*, *Eur. Phys. J. C* **78** (2018) 317 [arXiv:1803.00950] [INSPIRE].

[14] ATLAS collaboration, *Measurement of the top-quark mass in $t\bar{t}$ + 1-jet events collected with the ATLAS detector in pp collisions at $\sqrt{s} = 8$ TeV*, *JHEP* **11** (2019) 150 [arXiv:1905.02302] [INSPIRE].

[15] CMS collaboration, *Measurement of the cross section for $t\bar{t}$ production with additional jets and b jets in pp collisions at $\sqrt{s} = 13$ TeV*, *JHEP* **07** (2020) 125 [arXiv:2003.06467] [INSPIRE].

[16] T. Gehrmann, J.M. Henn and N.A. Lo Presti, *Analytic form of the two-loop planar five-gluon all-plus-helicity amplitude in QCD*, *Phys. Rev. Lett.* **116** (2016) 062001 [arXiv:1511.05409] [INSPIRE].

[17] C.G. Papadopoulos, D. Tommasini and C. Wever, *The Pentabox Master Integrals with the Simplified Differential Equations approach*, *JHEP* **04** (2016) 078 [arXiv:1511.09404] [INSPIRE].

[18] T. Gehrmann, J.M. Henn and N.A. Lo Presti, *Pentagon functions for massless planar scattering amplitudes*, *JHEP* **10** (2018) 103 [arXiv:1807.09812] [INSPIRE].

[19] S. Abreu, L.J. Dixon, E. Herrmann, B. Page and M. Zeng, *The two-loop five-point amplitude in $\mathcal{N} = 4$ super-Yang-Mills theory*, *Phys. Rev. Lett.* **122** (2019) 121603 [arXiv:1812.08941] [INSPIRE].

[20] D. Chicherin, T. Gehrmann, J.M. Henn, P. Wasser, Y. Zhang and S. Zoia, *All Master Integrals for Three-Jet Production at Next-to-Next-to-Leading Order*, *Phys. Rev. Lett.* **123** (2019) 041603 [arXiv:1812.11160] [INSPIRE].

JHEP01(2023)156

[21] D. Chicherin and V. Sotnikov, *Pentagon Functions for Scattering of Five Massless Particles*, *JHEP* **20** (2020) 167 [arXiv:2009.07803] [INSPIRE].

[22] S. Abreu, H. Ita, F. Moriello, B. Page, W. Tschernow and M. Zeng, *Two-Loop Integrals for Planar Five-Point One-Mass Processes*, *JHEP* **11** (2020) 117 [arXiv:2005.04195] [INSPIRE].

[23] D.D. Canko, C.G. Papadopoulos and N. Syrrakos, *Analytic representation of all planar two-loop five-point Master Integrals with one off-shell leg*, *JHEP* **01** (2021) 199 [arXiv:2009.13917] [INSPIRE].

[24] D. Chicherin, V. Sotnikov and S. Zoia, *Pentagon functions for one-mass planar scattering amplitudes*, *JHEP* **01** (2022) 096 [arXiv:2110.10111] [INSPIRE].

[25] S. Abreu, H. Ita, B. Page and W. Tschernow, *Two-loop hexa-box integrals for non-planar five-point one-mass processes*, *JHEP* **03** (2022) 182 [arXiv:2107.14180] [INSPIRE].

[26] S. Badger, C. Brønnum-Hansen, H.B. Hartanto and T. Peraro, *Analytic helicity amplitudes for two-loop five-gluon scattering: the single-minus case*, *JHEP* **01** (2019) 186 [arXiv:1811.11699] [INSPIRE].

[27] D. Chicherin, T. Gehrmann, J.M. Henn, P. Wasser, Y. Zhang and S. Zoia, *Analytic result for a two-loop five-particle amplitude*, *Phys. Rev. Lett.* **122** (2019) 121602 [arXiv:1812.11057] [INSPIRE].

[28] S. Abreu, J. Dormans, F. Febres Cordero, H. Ita and B. Page, *Analytic Form of Planar Two-Loop Five-Gluon Scattering Amplitudes in QCD*, *Phys. Rev. Lett.* **122** (2019) 082002 [arXiv:1812.04586] [INSPIRE].

[29] S. Abreu, J. Dormans, F. Febres Cordero, H. Ita, B. Page and V. Sotnikov, *Analytic Form of the Planar Two-Loop Five-Parton Scattering Amplitudes in QCD*, *JHEP* **05** (2019) 084 [arXiv:1904.00945] [INSPIRE].

[30] S. Abreu, F. Febres Cordero, H. Ita, B. Page and V. Sotnikov, *Planar Two-Loop Five-Parton Amplitudes from Numerical Unitarity*, *JHEP* **11** (2018) 116 [arXiv:1809.09067] [INSPIRE].

[31] S. Badger, D. Chicherin, T. Gehrmann, G. Heinrich, J.M. Henn, T. Peraro et al., *Analytic form of the full two-loop five-gluon all-plus helicity amplitude*, *Phys. Rev. Lett.* **123** (2019) 071601 [arXiv:1905.03733] [INSPIRE].

[32] S. Abreu, B. Page, E. Pascual and V. Sotnikov, *Leading-Color Two-Loop QCD Corrections for Three-Photon Production at Hadron Colliders*, *JHEP* **01** (2021) 078 [arXiv:2010.15834] [INSPIRE].

[33] S. Abreu, F. Febres Cordero, H. Ita, B. Page and V. Sotnikov, *Leading-color two-loop QCD corrections for three-jet production at hadron colliders*, *JHEP* **07** (2021) 095 [arXiv:2102.13609] [INSPIRE].

[34] H.A. Chawdhry, M. Czakon, A. Mitov and R. Poncelet, *Two-loop leading-color helicity amplitudes for three-photon production at the LHC*, *JHEP* **06** (2021) 150 [arXiv:2012.13553] [INSPIRE].

[35] H.B. Hartanto, S. Badger, C. Brønnum-Hansen and T. Peraro, *A numerical evaluation of planar two-loop helicity amplitudes for a W-boson plus four partons*, *JHEP* **09** (2019) 119 [arXiv:1906.11862] [INSPIRE].

[36] B. Agarwal, F. Buccioni, A. von Manteuffel and L. Tancredi, *Two-loop leading colour QCD corrections to $q\bar{q} \to \gamma\gamma g$ and $qg \to \gamma\gamma q$*, *JHEP* **04** (2021) 201 [arXiv:2102.01820] [INSPIRE].

JHEP01(2023)156

[37] H.A. Chawdhry, M. Czakon, A. Mitov and R. Poncelet, *Two-loop leading-colour QCD helicity amplitudes for two-photon plus jet production at the LHC*, *JHEP* **07** (2021) 164 [arXiv:2103.04319] [INSPIRE].

[38] B. Agarwal, F. Buccioni, A. von Manteuffel and L. Tancredi, *Two-Loop Helicity Amplitudes for Diphoton Plus Jet Production in Full Color*, *Phys. Rev. Lett.* **127** (2021) 262001 [arXiv:2105.04585] [INSPIRE].

[39] S. Badger, C. Brønnum-Hansen, D. Chicherin, T. Gehrmann, H.B. Hartanto, J. Henn et al., *Virtual QCD corrections to gluon-initiated diphoton plus jet production at hadron colliders*, *JHEP* **11** (2021) 083 [arXiv:2106.08664] [INSPIRE].

[40] S. Badger, H.B. Hartanto, J. Kryś and S. Zoia, *Two-loop leading-colour QCD helicity amplitudes for Higgs boson production in association with a bottom-quark pair at the LHC*, *JHEP* **11** (2021) 012 [arXiv:2107.14733] [INSPIRE].

[41] S. Badger, H.B. Hartanto, J. Kryś and S. Zoia, *Two-loop leading colour helicity amplitudes for $W^{\pm}\gamma + j$ production at the LHC*, *JHEP* **05** (2022) 035 [arXiv:2201.04075] [INSPIRE].

[42] H.A. Chawdhry, M.L. Czakon, A. Mitov and R. Poncelet, *NNLO QCD corrections to three-photon production at the LHC*, *JHEP* **02** (2020) 057 [arXiv:1911.00479] [INSPIRE].

[43] S. Kallweit, V. Sotnikov and M. Wiesemann, *Triphoton production at hadron colliders in NNLO QCD*, *Phys. Lett. B* **812** (2021) 136013 [arXiv:2010.04681] [INSPIRE].

[44] H.A. Chawdhry, M. Czakon, A. Mitov and R. Poncelet, *NNLO QCD corrections to diphoton production with an additional jet at the LHC*, *JHEP* **09** (2021) 093 [arXiv:2105.06940] [INSPIRE].

[45] S. Badger, T. Gehrmann, M. Marcoli and R. Moodie, *Next-to-leading order QCD corrections to diphoton-plus-jet production through gluon fusion at the LHC*, *Phys. Lett. B* **824** (2022) 136802 [arXiv:2109.12003] [INSPIRE].

[46] H.B. Hartanto, R. Poncelet, A. Popescu and S. Zoia, *Next-to-next-to-leading order QCD corrections to $Wb\bar{b}$ production at the LHC*, *Phys. Rev. D* **106** (2022) 074016 [arXiv:2205.01687] [INSPIRE].

[47] A.V. Kotikov, *Differential equations method: New technique for massive Feynman diagrams calculation*, *Phys. Lett. B* **254** (1991) 158 [INSPIRE].

[48] E. Remiddi, *Differential equations for Feynman graph amplitudes*, *Nuovo Cim. A* **110** (1997) 1435 [hep-th/9711188] [INSPIRE].

[49] J.M. Henn, *Multiloop integrals in dimensional regularization made simple*, *Phys. Rev. Lett.* **110** (2013) 251601 [arXiv:1304.1806] [INSPIRE].

[50] F.V. Tkachov, *A Theorem on Analytical Calculability of Four Loop Renormalization Group Functions*, *Phys. Lett. B* **100** (1981) 65 [INSPIRE].

[51] K.G. Chetyrkin and F.V. Tkachov, *Integration by Parts: The Algorithm to Calculate beta Functions in 4 Loops*, *Nucl. Phys. B* **192** (1981) 159 [INSPIRE].

[52] S. Laporta, *High precision calculation of multiloop Feynman integrals by difference equations*, *Int. J. Mod. Phys. A* **15** (2000) 5087 [hep-ph/0102033] [INSPIRE].

[53] A. von Manteuffel and R.M. Schabinger, *A novel approach to integration by parts reduction*, *Phys. Lett. B* **744** (2015) 101 [arXiv:1406.4513] [INSPIRE].

[54] T. Peraro, *Scattering amplitudes over finite fields and multivariate functional reconstruction*, *JHEP* **12** (2016) 030 [arXiv:1608.01902] [INSPIRE].

JHEP01(2023)156

[55] T. Peraro, *FiniteFlow: multivariate functional reconstruction using finite fields and dataflow graphs*, *JHEP* **07** (2019) 031 [arXiv:1905.08019] [INSPIRE].

[56] R.N. Lee, A.V. Smirnov and V.A. Smirnov, *Solving differential equations for Feynman integrals by expansions near singular points*, *JHEP* **03** (2018) 008 [arXiv:1709.07525] [INSPIRE].

[57] M.K. Mandal and X. Zhao, *Evaluating multi-loop Feynman integrals numerically through differential equations*, *JHEP* **03** (2019) 190 [arXiv:1812.03060] [INSPIRE].

[58] F. Moriello, *Generalised power series expansions for the elliptic planar families of Higgs + jet production at two loops*, *JHEP* **01** (2020) 150 [arXiv:1907.13234] [INSPIRE].

[59] M. Hidding, *DiffExp, a Mathematica package for computing Feynman integrals in terms of one-dimensional series expansions*, *Comput. Phys. Commun.* **269** (2021) 108125 [arXiv:2006.05510] [INSPIRE].

[60] X. Liu, Y.-Q. Ma and C.-Y. Wang, *A Systematic and Efficient Method to Compute Multi-loop Master Integrals*, *Phys. Lett. B* **779** (2018) 353 [arXiv:1711.09572] [INSPIRE].

[61] X. Liu and Y.-Q. Ma, *Multiloop corrections for collider processes using auxiliary mass flow*, *Phys. Rev. D* **105** (2022) L051503 [arXiv:2107.01864] [INSPIRE].

[62] Z.-F. Liu and Y.-Q. Ma, *Automatic computation of Feynman integrals containing linear propagators via auxiliary mass flow*, *Phys. Rev. D* **105** (2022) 074003 [arXiv:2201.11636] [INSPIRE].

[63] X. Liu and Y.-Q. Ma, *AMFlow: A Mathematica package for Feynman integrals computation via auxiliary mass flow*, *Comput. Phys. Commun.* **283** (2023) 108565 [arXiv:2201.11669] [INSPIRE].

[64] R. Bonciani, V. Del Duca, H. Frellesvig, J.M. Henn, F. Moriello and V.A. Smirnov, *Two-loop planar master integrals for Higgs→ 3 partons with full heavy-quark mass dependence*, *JHEP* **12** (2016) 096 [arXiv:1609.06685] [INSPIRE].

[65] R. Bonciani, V. Del Duca, H. Frellesvig, J.M. Henn, M. Hidding, L. Maestri et al., *Evaluating a family of two-loop non-planar master integrals for Higgs + jet production with full heavy-quark mass dependence*, *JHEP* **01** (2020) 132 [arXiv:1907.13156] [INSPIRE].

[66] H. Frellesvig, M. Hidding, L. Maestri, F. Moriello and G. Salvatori, *The complete set of two-loop master integrals for Higgs + jet production in QCD*, *JHEP* **06** (2020) 093 [arXiv:1911.06308] [INSPIRE].

[67] M. Becchetti, R. Bonciani, V. Del Duca, V. Hirschi, F. Moriello and A. Schweitzer, *Next-to-leading order corrections to light-quark mixed QCD-EW contributions to Higgs boson production*, *Phys. Rev. D* **103** (2021) 054037 [arXiv:2010.09451] [INSPIRE].

[68] T. Armadillo, R. Bonciani, S. Devoto, N. Rana and A. Vicini, *Two-loop mixed QCD-EW corrections to neutral current Drell-Yan*, *JHEP* **05** (2022) 072 [arXiv:2201.01754] [INSPIRE].

[69] R. Bonciani, L. Buonocore, M. Grazzini, S. Kallweit, N. Rana, F. Tramontano et al., *Mixed Strong-Electroweak Corrections to the Drell-Yan Process*, *Phys. Rev. Lett.* **128** (2022) 012002 [arXiv:2106.11953] [INSPIRE].

[70] S. Badger, M. Becchetti, E. Chaubey, R. Marzucca and F. Sarandrea, *One-loop QCD helicity amplitudes for $pp \to t\bar{t}j$ to $O(\varepsilon^2)$*, *JHEP* **06** (2022) 066 [arXiv:2201.12188] [INSPIRE].

[71] K.G. Chetyrkin, A.L. Kataev and F.V. Tkachov, *Higher Order Corrections to $\sigma_{\rm tot}(e^+e^- \to hadrons)$ in Quantum Chromodynamics*, *Phys. Lett. B* **85** (1979) 277 [INSPIRE].

JHEP01(2023)156

[72] R.N. Lee, *Presenting LiteRed: a tool for the Loop InTEgrals REDuction*, arXiv:1212.2685 [INSPIRE].

[73] R.N. Lee, *LiteRed 1.4: a powerful tool for reduction of multiloop integrals*, *J. Phys. Conf. Ser.* **523** (2014) 012059 [arXiv:1310.1145] [INSPIRE].

[74] N. Arkani-Hamed, J.L. Bourjaily, F. Cachazo, S. Caron-Huot and J. Trnka, *The All-Loop Integrand For Scattering Amplitudes in Planar $N = 4$ SYM*, *JHEP* **01** (2011) 041 [arXiv:1008.2958] [INSPIRE].

[75] N. Arkani-Hamed, J.L. Bourjaily, F. Cachazo and J. Trnka, *Local Integrals for Planar Scattering Amplitudes*, *JHEP* **06** (2012) 125 [arXiv:1012.6032] [INSPIRE].

[76] S. Badger, G. Mogull and T. Peraro, *Local integrands for two-loop all-plus Yang-Mills amplitudes*, *JHEP* **08** (2016) 063 [arXiv:1606.02244] [INSPIRE].

[77] T. Gehrmann, A. von Manteuffel, L. Tancredi and E. Weihs, *The two-loop master integrals for $q\bar{q} \to VV$*, *JHEP* **06** (2014) 032 [arXiv:1404.4853] [INSPIRE].

[78] M. Argeri, S. Di Vita, P. Mastrolia, E. Mirabella, J. Schlenk, U. Schubert et al., *Magnus and Dyson Series for Master Integrals*, *JHEP* **03** (2014) 082 [arXiv:1401.2979] [INSPIRE].

[79] R.N. Lee, *Reducing differential equations for multiloop master integrals*, *JHEP* **04** (2015) 108 [arXiv:1411.0911] [INSPIRE].

[80] R.N. Lee, *Libra: A package for transformation of differential systems for multiloop integrals*, *Comput. Phys. Commun.* **267** (2021) 108058 [arXiv:2012.00279] [INSPIRE].

[81] O. Gituliar and V. Magerya, *Fuchsia: a tool for reducing differential equations for Feynman master integrals to epsilon form*, *Comput. Phys. Commun.* **219** (2017) 329 [arXiv:1701.04269] [INSPIRE].

[82] M. Prausa, *epsilon: A tool to find a canonical basis of master integrals*, *Comput. Phys. Commun.* **219** (2017) 361 [arXiv:1701.00725] [INSPIRE].

[83] C. Dlapa, J. Henn and K. Yan, *Deriving canonical differential equations for Feynman integrals from a single uniform weight integral*, *JHEP* **05** (2020) 025 [arXiv:2002.02340] [INSPIRE].

[84] C. Dlapa, X. Li and Y. Zhang, *Leading singularities in Baikov representation and Feynman integrals with uniform transcendental weight*, *JHEP* **07** (2021) 227 [arXiv:2103.04638] [INSPIRE].

[85] S. Abreu, B. Page and M. Zeng, *Differential equations from unitarity cuts: nonplanar hexa-box integrals*, *JHEP* **01** (2019) 006 [arXiv:1807.11522] [INSPIRE].

[86] D. Chicherin, T. Gehrmann, J.M. Henn, P. Wasser, Y. Zhang and S. Zoia, *The two-loop five-particle amplitude in $\mathcal{N} = 8$ supergravity*, *JHEP* **03** (2019) 115 [arXiv:1901.05932] [INSPIRE].

[87] S. Abreu, L.J. Dixon, E. Herrmann, B. Page and M. Zeng, *The two-loop five-point amplitude in $\mathcal{N} = 8$ supergravity*, *JHEP* **03** (2019) 123 [arXiv:1901.08563] [INSPIRE].

[88] L.-B. Chen and J. Wang, *Analytic two-loop master integrals for tW production at hadron colliders: I*, *Chin. Phys. C* **45** (2021) 123106 [arXiv:2106.12093] [INSPIRE].

[89] M. Heller, A. von Manteuffel and R.M. Schabinger, *Multiple polylogarithms with algebraic arguments and the two-loop EW-QCD Drell-Yan master integrals*, *Phys. Rev. D* **102** (2020) 016025 [arXiv:1907.00491] [INSPIRE].

JHEP01(2023)156

[90] S. Zoia, *Modern Analytic Methods for Computing Scattering Amplitudes: With Application to Two-Loop Five-Particle Processes*, Ph.D. Thesis, Department of Physics, University of Turin, Turin, Italy [DOI] [INSPIRE].

[91] E. Chaubey, M. Kaur and A. Shivaji, *Master integrals for $\mathcal{O}(\alpha\alpha_s)$ corrections to $H \to ZZ^*$*, *JHEP* **10** (2022) 056 [arXiv:2205.06339] [INSPIRE].

[92] D. Chicherin, J. Henn and V. Mitev, *Bootstrapping pentagon functions*, *JHEP* **05** (2018) 164 [arXiv:1712.09610] [INSPIRE].

[93] A.B. Goncharov, M. Spradlin, C. Vergu and A. Volovich, *Classical Polylogarithms for Amplitudes and Wilson Loops*, *Phys. Rev. Lett.* **105** (2010) 151605 [arXiv:1006.5703] [INSPIRE].

[94] C. Duhr, H. Gangl and J.R. Rhodes, *From polygons and symbols to polylogarithmic functions*, *JHEP* **10** (2012) 075 [arXiv:1110.0458] [INSPIRE].

[95] C. Duhr, *Hopf algebras, coproducts and symbols: an application to Higgs boson amplitudes*, *JHEP* **08** (2012) 043 [arXiv:1203.0454] [INSPIRE].

[96] C. Duhr and F. Dulat, *PolyLogTools — polylogs for the masses*, *JHEP* **08** (2019) 135 [arXiv:1904.07279] [INSPIRE].

[97] D. Gaiotto, J. Maldacena, A. Sever and P. Vieira, *Pulling the straps of polygons*, *JHEP* **12** (2011) 011 [arXiv:1102.0062] [INSPIRE].

[98] R. Bonciani, V. Del Duca, H. Frellesvig, M. Hidding, V. Hirschi, F. Moriello et al., *Next-to-leading-order QCD Corrections to Higgs Production in association with a Jet*, arXiv:2206.10490 [INSPIRE].

[99] D. Chicherin, J.M. Henn and G. Papathanasiou, *Cluster algebras for Feynman integrals*, *Phys. Rev. Lett.* **126** (2021) 091603 [arXiv:2012.12285] [INSPIRE].

[100] S. He, Z. Li and Q. Yang, *Notes on cluster algebras and some all-loop Feynman integrals*, *JHEP* **06** (2021) 119 [arXiv:2103.02796] [INSPIRE].

[101] H.S. Hannesdottir, A.J. McLeod, M.D. Schwartz and C. Vergu, *Implications of the Landau equations for iterated integrals*, *Phys. Rev. D* **105** (2022) L061701 [arXiv:2109.09744] [INSPIRE].

[102] J.L. Bourjaily, C. Vergu and M. von Hippel, *Landau Singularities and Higher-Order Roots*, arXiv:2208.12765 [INSPIRE].

[103] W. Flieger and W.J. Torres Bobadilla, *Landau and leading singularities in arbitrary space-time dimensions*, MPP-2022-129 (2022) [INSPIRE].

JHEP01(2023)156